

**Modeling the Flash Gate Board
for
Water Storage and Flood Control**

by
David Stephen Malyevac Jr.

Thesis submitted to the Faculty of the
Virginia Polytechnic Institute and State University
in partial fulfillment of the requirements for the degree of
Master of Science
in
Mechanical Engineering

APPROVED:

Dr. Robert G. Leonard, Chairman

Dr. Harry H. Robertshaw

Dr. Robert H. Fries

May, 1988
Blacksburg, Virginia

**Modeling the Flash Gate Board
for
Water Storage and Flood Control**

by

David Stephen Malyevac Jr.

Dr. Robert G. Leonard, Chairman

Mechanical Engineering

(ABSTRACT)

The height of an overflow dam must be designed low enough to prevent the reservoir water level from exceeding a flood plain during flooding conditions. Because of this constraint, much of the available water storage area is wasted and the available pressure head for power generation will be less than maximum during normal conditions. Crest control gates alleviate this problem by providing a variable spillway height. The Flash Gate Board is a passive automatic crest control gate. Its purpose is to regulate flood water while providing increased water pressure for power generation or for additional water storage for a municipality. The governing equations for the Flash Gate Board system are derived and used to formulate models of the system. Computer simulations are used to examine the system response in a variety of operating conditions. The results of these simulations are presented and discussed. The results include an investigation which developed an optimum gate height to maximize the potential of the Flash Gate Board. An experimental model was developed to verify analytical results and to provide additional insight. Conclusions from the study, recommendations for future work, and modifications for a trouble-free design are discussed.

To Cindy

Acknowledgements

I would like to thank Dr. Robertshaw and Dr. Fries for serving on my advisory committee and for the instruction and insight they have provided me in the classroom.

I would especially like to thank Dr. R. G. Leonard for serving as my advisor. Your support and guidance have been invaluable.

I would also like to thank all the people in the mechanical shop for their help in building the experimental model, especially Johnny Cox.

Thanks to all the members of the Wednesday control group for your suggestions and help.

Special thanks go to Mom and Dad for all their support and encouragement. You always believed in me, even when I didn't.

Finally, thanks to my wife, Cindy, without whom I never would have made it.

Table of Contents

1.0 Introduction	1
2.0 Review of Literature	5
2.1 Crest Control	5
2.2 Analysis of Crest Control Devices	9
3.0 Model Development	13
3.1 Introduction	13
3.2 Static Formulation	13
3.2.1 Ideal Hydrostatic Moment	14
3.2.2 Ideal Flow Discharge	17
3.2.3 Actual Moment and Flow Determination	20
3.2.4 Static Results	26
3.2.5 Spring Design	35
3.2.5.1 Torsion Bar Spring	37
3.2.5.2 Helical Torsion Spring	39
3.3 Dynamic Analysis	41
3.3.1 Rotational Equation of Motion	42
3.3.1.1 Virtual Inertia	43
3.3.1.2 Linear Spring	45
3.3.1.3 Headwater Moment	47
3.3.1.4 Viscous Damping Coefficient	48
3.3.1.5 Hydrodynamic Damping	48

3.3.2 Reservoir Dynamics	50
3.4 Dynamic Results	51
3.4.1 Fast Model	51
3.4.2 Slow Model	56
3.4.3 Optimum Gate Height	56
4.0 Experimental Analysis	66
4.1 Experimental Setup	66
4.2 Operation of Experiment	67
4.3 Experimental Results and Observations	69
5.0 Conclusions and Recommendations	71
References	76
Vita	78

List of Illustrations

Figure 1. Idealized Flash Gate Board System	2
Figure 2. Typical Flashboard Installation	6
Figure 3. Hinged-leaf gates	8
Figure 4. Freebody diagram of Flash Gate Board	15
Figure 5. Flash Gate Board with parallel flow	18
Figure 6. Empirical discharge coefficients	22
Figure 7. Actual and Ideal flow over horizontal gate	23
Figure 8. Calculated moment coefficients vs. gate angle	25
Figure 9. Typical pier types	27
Figure 10. Theoretical moment vs. water height for fixed gate angles	28
Figure 11. Theoretical discharge vs. water height for fixed gate angles	30
Figure 12. Actual moment vs. water height for fixed gate angles	31
Figure 13. Actual discharge vs. water height for fixed gate angles	32
Figure 14. Results of linear theta design vs. water height	33
Figure 15. Results of quadratic theta design vs. water height	34
Figure 16. Gate angle vs. water height for linear springs	36
Figure 17. Typical torsion bar spring	38
Figure 18. Helical torsion spring with round cross section	40
Figure 19. Freebody diagram of the Flash Gate Board system	44
Figure 20. Added inertia for general gate position	46
Figure 21. Block diagram of third order dynamic model	52
Figure 22. System response to impulse input	54
Figure 23. Contribution of each term in Equation 3.27	55
Figure 24. Three water level response to impulse	57
Figure 25. First order model response to rain input 1	58

Figure 26. First order model response to rain input 2 59

Figure 27. Gate angle vs. water height for gate height to flood right ratios 61

Figure 28. Verification of optimum gate height as limit before bang-bang 63

Figure 29. Iteration to find dynamic optimum gate height 65

Figure 30. Exploded view of experiment components 68

List of Tables

Table 1. Discharge coefficient curve fit results 21

Table 2. Moment coefficient curve fit results 24

Table 3. Results of torsion bar stress analysis 37

Nomenclature

The following symbols have been used in this work

A	Reservoir area
C_d	Discharge coefficient
C_{drag}	Hydrodynamic drag coefficient
C_m	Moment coefficient
FR	Flood rights level, assumed to be height of water that maintains gate in its full open position
GH	Height of Flash Gate Board
H_d	Design head of reservoir
J_v	Virtual moment of inertia of gate
K_t	Linear spring rate
M_d	Moment from hydrodynamic drag
M_r	Moment of restoring spring
M_w	Moment at gate pin due to headwater pressure
$P(y)$	Hydrostatic pressure distribution
Q	Volumetric flow discharge over the gate
Q_{in}	Volumetric flow input to reservoir (rain and drainage)
V	Upstream water velocity of approach
\bar{V}	Average velocity of gate
b	Crest length of Flash Gate Board
g	Acceleration of gravity (32.174 ft / sec ²)
h	Reservoir height above dam (from base of Flash Gate Board)
\bar{h}	Height of water above crest of gate

h_{tot}	Total head at gate
h_v	Velocity head
γ	Specific density of water (62.4 lb _m / ft ³)
θ	Gate angle from vertical
ζ	Damping ratio

1.0 Introduction

Dams retain water for water supplies, flood control, irrigation, navigation, recreation and/or for hydroelectric power generation. All dams must have a provision for passing the portion of inflow to the reservoir that cannot be stored or used immediately. For overflow dams the excess water passes over a spillway. A spillway is a surface over which water from the top of the reservoir flows to the tailwater level downstream.

The dam and spillway are designed to maintain a given water level during normal conditions constraining water to a fixed geographical area. During heavy rainfalls or spring snow melts the dam and spillway must be designed to pass the excess water without allowing the water depth in the reservoir behind the dam to exceed a depth defined as the flood rights. The flood rights protect adjoining property from water damage during flood conditions.

The spillway of an overflow dam must be designed low enough so that during flood conditions the reservoir water level will not exceed flood rights level. Because of this constraint, much of the available water storage area is wasted, and the pressure head at the dam will be less than maximum during normal conditions. One solution to this problem is to provide a variable spillway height. This is the purpose of the Flash Gate Board, the subject of this investigation.

The Flash Gate Board is a passive automatic water control gate to be mounted on the crest of an overflow dam. The purpose of the Flash Gate Board is to increase the storage volume of a new or existing reservoir and provide increased head for power generation while maintaining the water depth at the flood rights level during flooding conditions. The Flash Gate Board, see Figure 1, is a spring-loaded hinged-leaf type crest control gate. At normal conditions the gate is held in an

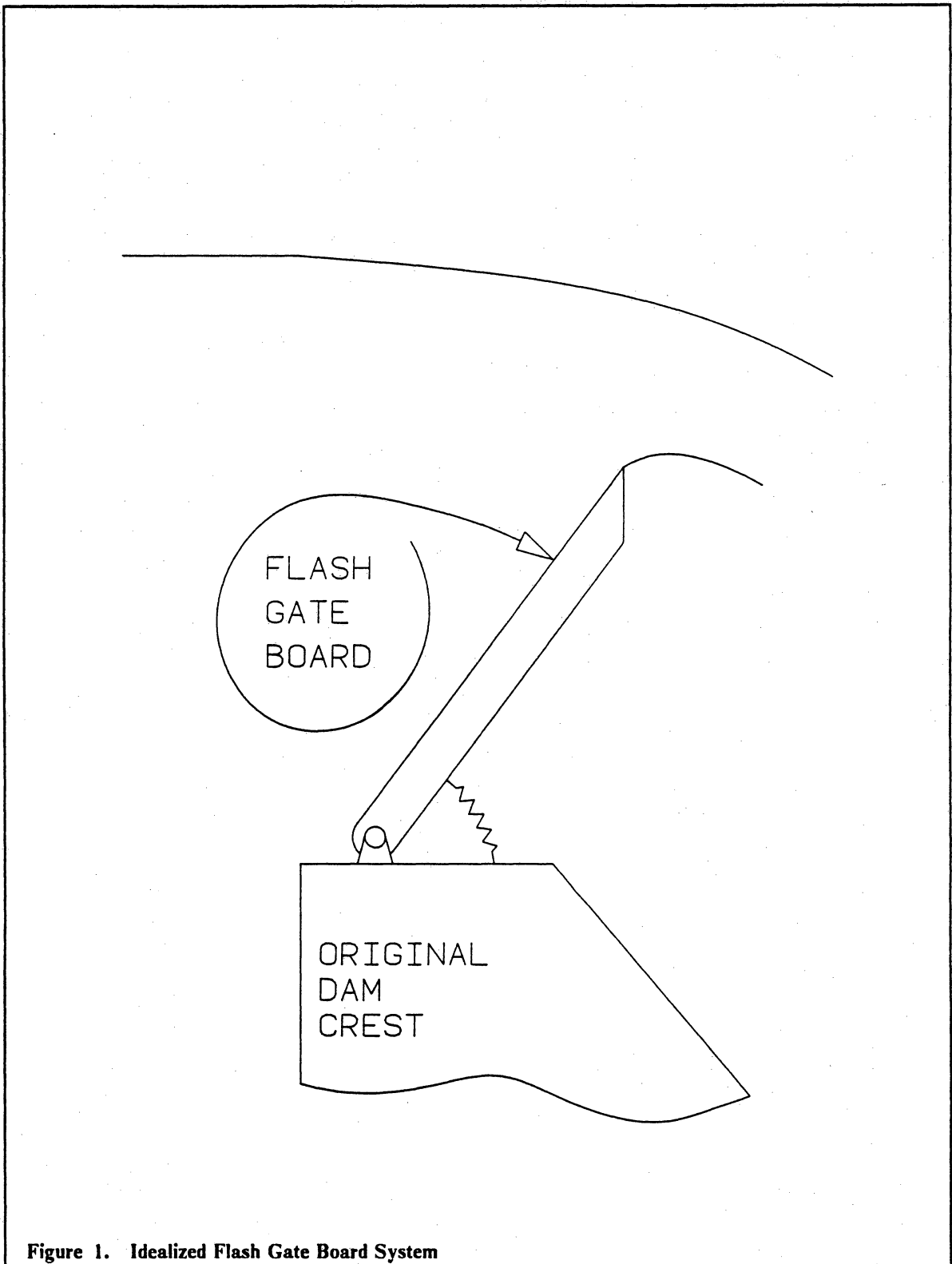


Figure 1. Idealized Flash Gate Board System

upright or near upright position increasing the spillway height of the dam. During conditions of heavy rainfall or flood conditions, the Flash Gate Board lowers due to the increase in hydrostatic pressure of the increasing water height. Then more storm water is allowed to pass. When the water height reaches the maximum design flood level, flood rights level, the gate is horizontal and the original dam spillway height is in effect.

An evaluation performed by the United States Department of Commerce, using data from 1985, projects that if the Flash Gate Board is added to 10 % of the possible available sites, the annual increase in electrical energy would be approximately 1 billion Kwh. This is equivalent to burning 1.75 million barrels of oil annually at 35 % efficiency (Mcquire, 1986 [11]¹). These savings are conservative and only include the hydroelectric potential savings. In addition are the water reserve savings. Although the cost analysis done was only a rough approximation, it appears as though the Flash Gate Board has the potential for being a valuable asset in energy related industries.

Given the potential economic benefits of the Flash Gate Board, the purpose of this investigation is to formulate a dynamic model of the Flash Gate Board system. The model is then to be used to determine the system response to a variety of inputs. These inputs range from sudden log impact, to normal and abnormal rainfall patterns.

This report will summarize the pertinent literature available on crest control gates. Next, the report will present the derivation of the governing equations for the Flash Gate Board system. These equations were used to perform a computer simulation of the system. The results of this simulation are presented and discussed. An experimental model is proposed to verify and add additional insight to the problem. The results of this experimental model are presented and compared to those obtained from the analytical study.

¹ Numbers in brackets indicate reference numbers.

Also considered in this investigation are causes and solutions for possible vibration problems and the determination of an optimum gate height for a given reservoir. A software package to facilitate a designer in the location-specific design was developed. An evaluation of various spring designs and configurations is also presented.

Finally, conclusions are drawn on the usefulness of this type of crest control gate. Recommendations for future work and possible improvements to the design are made.

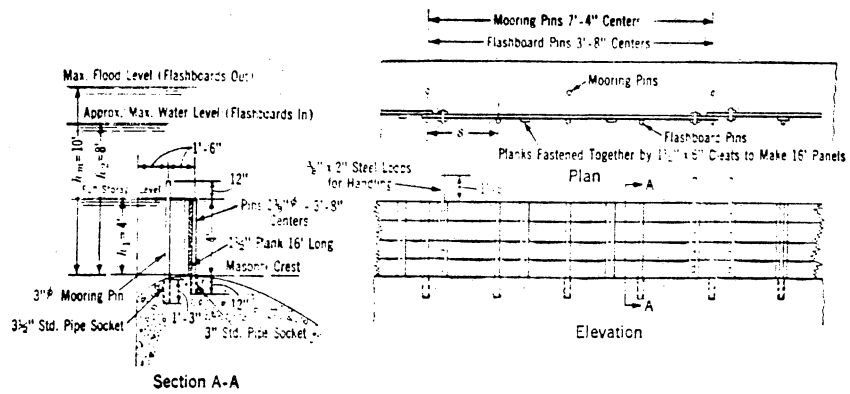
2.0 Review of Literature

The literature reviewed for this project can be broken into two main themes. Therefore this chapter has been divided into two parts. The first part is concerned with the other types of crest control devices that are used and have been used. The second part describes the work that has been done on the analysis of these types of structures.

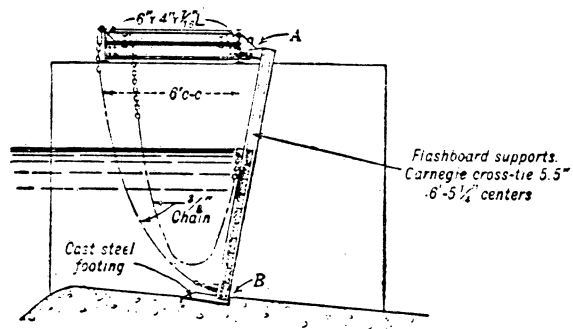
2.1 *Crest Control*

Crest control is usually defined as the form of spillway control that raises the effective crest level of the dam. This provides a means of regulating the flow over the surface of the device. This type of spillway control generally makes use of the headwater pressure for actuation and regulation of the discharge.

There have been many approaches to the problem of a variable spillway height. The simplest and probably the oldest form of crest control are temporary flashboards. Flashboards are a series of wooden planks or boards installed on the crest of an overflow dam to raise the reservoir water level. Figure 2 shows a typical temporary flashboard installation. Temporary flashboards are supported by pins placed in sockets installed in the crest of the dam. The pins are designed to fail as the reservoir level "reaches" or "nears" the flood rights level. When the pins fail, the flashboards are released and the original dam passes the flood water.



Temporary Flashboards



Permanent Flashboards

Copied from (Creager, 1928 [5])

Figure 2. Typical Flashboard Installation

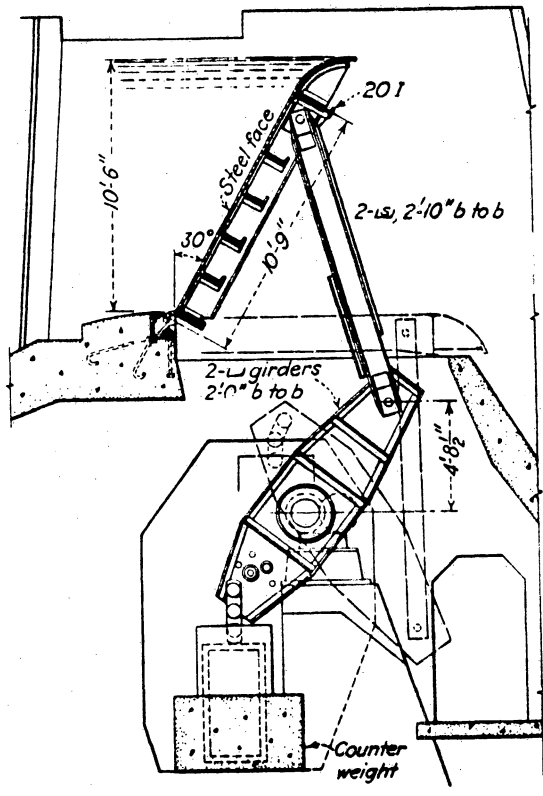
Flashboards have been used up to a height of 10 feet. There are problems with temporary flashboards in areas where floods occur suddenly and unexpectedly causing the flashboards to be washed out and lost. Replacing the flashboards several times a year is expensive.

Permanent flashboards are similar in design to the temporary flashboards. However, with permanent flashboards, the frame of the structure is not destroyed by storm flows. Permanent flashboards are held together by a series of steel framed sections mounted on the crest of the dam. An overhead crane raises and lowers the framed sections as water conditions require. Figure 2 shows a typical permanent flashboard installation.

Hinged-leaf gates are an improvement over the previously mentioned devices. The gate is a flat leaf hinged at the crest of the dam. When in an upright position, the gate adds to the spillway height. When lowered, the gate is horizontal and the spillway height required to pass flood water is maintained. The gate position is controlled manually by an overhead crane or automatically by a counterweight arrangement. Two types of hinged-leaf gates are shown in Figure 3.

Davis (Davis, 1969 [7]), suggests that this type of gate is well suited for use as a regulating gate and for passing debris. He points out, however, that for automatic operation the bearings and fulcrum point must be carefully designed and constructed. From his experience, corrosion has an adverse effect on the sensitivity of gate operation and can cause the water height for a necessary gate position to be several times the calculated value.

A more elaborate class of crest control is vertical lift gates. Vertical lift gates are usually used in larger installations where it necessary to store larger volumes of water. The higher forces required prohibit the use of the smaller, simpler gates mentioned above. Taintor-gates are the most widely used of the vertical lift gates. The gate section is a circular sector supported along its centerline by large bearings. It is rotated to open and close. The circular design of the Taintor-gate reduces the high opening and closing forces usually associated with vertical lift gates. This form of crest control is not directly comparable with the Flash Gate Board. However, Taintor-gates discharge water



Copied from (Davis, 1969 [7])

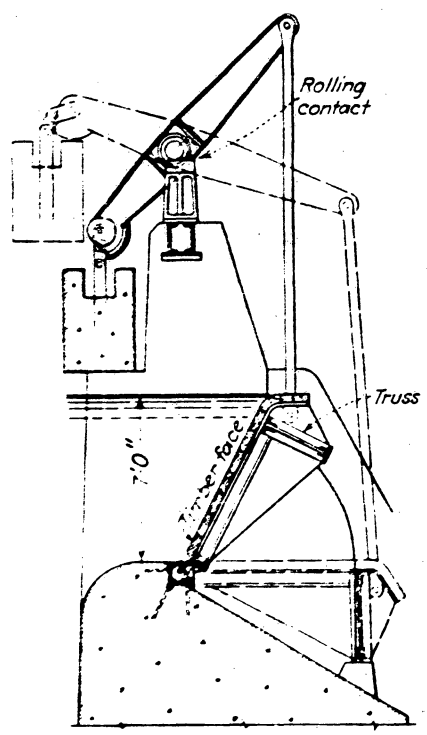


Figure 3. Hinged-leaf gates

under the gate and thus have problems with surface regulation and passage of debris. They are mentioned here because Taintor-gates may be retro-fitted with a Flash Gate Board to alleviate these problems.

The preceding discussion provides only an overview of crest control devices. A more detailed explanation of the types of control presented here along with descriptions of other types of control devices can be found in references [5], [6], and [7].

2.2 Analysis of Crest Control Devices

There is a limited amount of literature on the analysis of crest control devices similar to the Flash Gate Board. The literature that was reviewed tended to focus on flow-induced vibrations with emphasis on underflow gates. Papers that examined flow-induced vibrations on a general level as well as specific papers that analyze the phenomenon of nappe oscillation, flap gate oscillation due to nappe oscillation, and seal vibrations were also reviewed. Finally, literature relating to waves and vibration due to wave effects were briefly examined. While the literature reviewed cannot be directly applied to the derivation of the analytical model of the Flash Gate Board, it provided valuable insight into specific design considerations that must be considered in the final design of the device. This literature also provided a basis on which assumptions were made in the model development.

Of the papers reviewed, the best treatment of vibrations of hydraulic structures was provided by Kolkman (Kolkman, 1979 [11] and Novak, 1984 [16]). His focus is mainly on the general theoretical analysis of these structures. He then applies his theoretical analysis to specific examples, most of which involve gates with underflow and the induced vibrations from the underflowing water. Although his main focus is not on overflow type gates, he does, however, mention that the main

cause of vibration in overflow gates is due to the oscillation of the free stream (called the nappe) of water flowing over the gate. This is called nappe oscillation.

Schwartz (Schwartz, 1964 [21]) analyzes the phenomenon of nappe oscillation in general. He seeks to explain the mechanism of nappe oscillation. His theory suggests that the oscillation frequency is a function of the effective stiffness of the air trapped under the nappe. Using his theory, he determines a range of possible oscillation frequencies. He points out that the troublesome phenomenon of nappe oscillation can be suppressed with the additions of nappe splitters or spoilers. He stipulates that splitter spacing is dependant on the height of fall of the nappe.

Ogihara (Ogihara, 1979 [17] and 1977 [8]) suggests that the trapped air under the nappe acts as an air spring inducing vibrations in the gate. To eliminate this problem, like Schwartz, he suggests the addition of nappe splitters on the crest of the gate. The nappe splitters separate the overflowing water thus ventilating the trapped air under the nappe. He reports results from field experiments of flap gate oscillation of frequencies around 4 Hz with amplitudes up to 1.8 mm. Ogihara developed a new type of spoiler that is attached to the top of the flap gate to prevent these oscillations. Field tests with the new spoiler were successful in eliminating the vibration problem for the gates he studied.

Kolkman also was successful in eliminating flap gate oscillations using nappe splitters. He, however, points out that with thin oscillating nappes, more aeration is needed to prevent oscillations caused by pressure fluctuations. This may be an explanation as to why the Army Corp of Engineers (Nelson, 1979 [15]), was unsuccessful in eliminating a vibration problem on a flap gate using nappe splitters. It is not clear whether the nappe splitters used in both cases are comparable. Kolkman suggests that another means of providing ventilation of the nappe is through aeration pipes.

These results indicate the importance of a ventilated nappe. Therefore, in the development of a model for the Flash Gate Board, nappe ventilation was assumed. When a specific installation does

not allow for natural ventilation of the nappe, some form of artificially ventilating the nappe must be employed.

Another factor considered in the literature is that of proper design of the gate seals to avoid instabilities caused by seal vibrations. Kolkman suggests seals can provoke severe vibrations when a small leakage gap from wear and deformation appears. Rubber J-seals, named for the J-shape of their cross section, are common types of side seals. When the side seals are not in full contact with the pier plate, the resulting gap sets up pressure fluctuations that cause the seals to flutter. Schmidgal (Schmidgal, 1972 [20]) suggests that this seal vibration is caused by an exchange of static and dynamic forces on the seal.

Petukat (Petukat, 1979 [18]) further explains that self-excited seal vibrations are caused due to pressure variations at the seal gap. The water velocity through the gap consequently changes, thus compounding the pressure variations initiating the self-excited seal vibrations. Schmidgal points out from his experience with Taintor-gates that although the side seal vibration causes an audible hum, no severe effects on gate vibrations are noted. After encountering difficulties with proper alignment and adjustment of the standard side seal, Schmidgal proposes a redesigned J-seal to eliminate leakage and fluttering problems with the standard seal. Although his new seal has yet to be tested, he projects the redesign will maintain a positive side seal with gate gap variations up to 1.5 inch.

Petukat provides a thorough analysis of all types of seals. Of particular interest to this work was his work on vibration of bottom seals on flap gates. Vibrations of the bottom seal occur when sand is washed between the sealing plate and seal due to inaccurate construction. This caused the seal to be lifted up slightly inducing vibrations in the free end which in turn caused the entire seal to vibrate. The problem of possible seal vibration must be considered when choosing the side and bottom seals of the Flash Gate Board.

Also addressed in the literature is the issue of instabilities due to wave effects. Imaichi (Imaichi, 1977 [9]) investigated the instabilities in idealized Tainter-gate systems due to wave effects. Pickrill (Pickrill 1978 [19]) compares boat waves to wind waves and their effects on shorelines. This study provides general results on wind and boat generated waves. Pickrill shows that the maximum wave height of a boat generated wave is primarily dependant on the speed of the boat in contrast to its size or shape. Wind generated waves on the other hand, are dependant on the fetch (effective water surface area wind acts on) and on wind speed and duration. Pickrill discusses and compares the effects of both wind and boat waves on shorelines. Based on Pickrill's findings it appears the frequency of wind waves is much greater than the natural frequency of the Flash Gate Board system and thus should not present a problem. However, the instabilities resulting from waves is beyond the scope of this work and is presented here only as a possible reference for future work.

3.0 Model Development

3.1 *Introduction*

The derivation of a mathematical model of the Flash Gate Board required that all steady and transient forces on the system be determined. The equations representing these forces and the resulting moments tend to be non-linear and contain empirical coefficients that must be estimated or experimentally determined. The development of these equations is outlined and the results of simulations using these equations are presented. First the static equations are derived and the results are used to predict the static behavior of the Flash Gate Board. Next, the governing differential equations of motion of the system are derived. These equations form the framework for the dynamic simulation that is used to study the system's response. The simulation is used to predict the dynamic response of the system to a variety of inputs. The results of these simulations are presented and discussed.

3.2 *Static Formulation*

In order to study the static behavior of the Flash Gate Board an expression for the flow rate over the gate and the moment at the gate pin caused by headwater pressure were determined. Theoretical equations were first derived and empirical results applied to determine the actual equations. The development of the theoretical and actual equations for moment and flow are presented. The

static equations are used to predict the static behavior of the gate for fixed gate angles and to investigate the restoring spring requirements for given static gate angle versus water height profiles. Based on the results of this investigation, two designs for restoring spring are presented.

3.2.1 Ideal Hydrostatic Moment

The ideal hydrostatic moment at the gate pin is found by neglecting flow effects and integrating the hydraulic pressure distribution over the gate area. In the absence of flow effects, the ideal moment is the theoretical maximum moment due to the headwater hydrostatic pressure distribution on the gate. The moment at the gate pin due to headwater pressure is a function of the reservoir water height, the Flash Gate Board gate length, width, and gate angle.

The general gate position used to determine the moment due to the headwater pressure is shown in Figure 4. The differential force on the gate is:

$$dF = P(y) dA \quad (3.1)$$

Where dA is the differential gate area and $P(y)$ represents the headwater pressure distribution on the upper face of the gate. The pressure distribution is assumed to be hydrostatic. Therefore, referring to Figure 4, $P(y)$ is given by:

$$P(y) = \gamma (H - y \cos \theta) \quad (3.2)$$

The differential gate area, dA , is simply the gate length times the differential gate height, or:

$$dA = b dy \quad (3.3)$$

The hydrostatic force on the gate is then found by substituting equation (3.2) and (3.3) into equation (3.1) and integrating over the gate area:

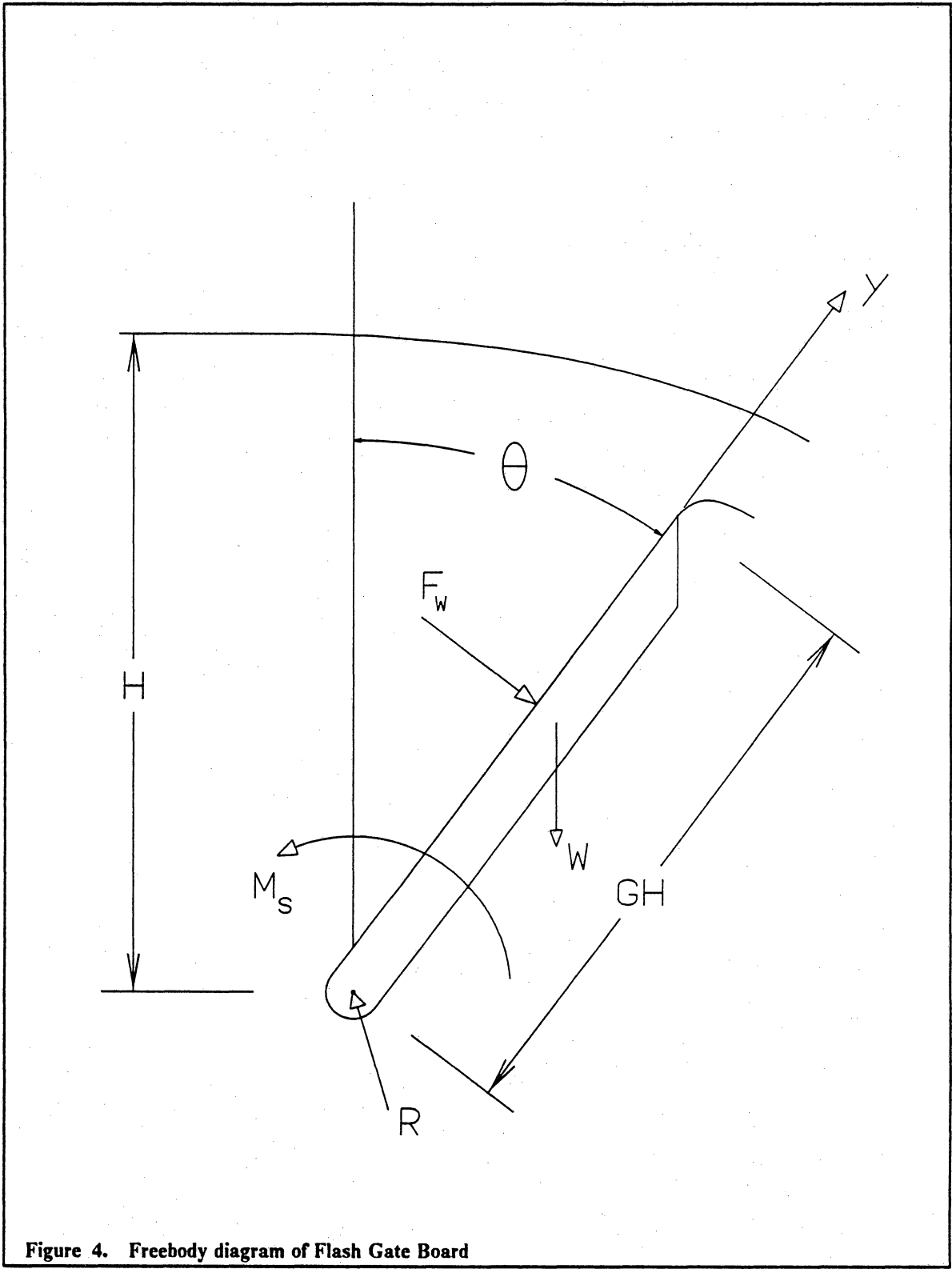


Figure 4. Freebody diagram of Flash Gate Board

$$F = \int_A \gamma (h - y \cos \theta) b dy \quad (3.4)$$

The upper limit of integration is different depending on whether or not the water height is above or below the top of the gate. For a water height below the top of the gate the integration is performed up to the water level on the gate. When the water is above the gate the integration is performed along the entire length of the gate. Then for water height below the top of the gate:

$$\begin{aligned} F &= b \gamma \int_0^{\frac{h}{\cos \theta}} (h - y \cos \theta) dy \\ &= \frac{b \gamma h^2}{2 \cos \theta} \end{aligned} \quad (3.5)$$

and for water height above the top of the gate:

$$\begin{aligned} F &= b \gamma \int_0^{GH} (h - y \cos \theta) dy \\ &= b \gamma GH \left[h - \frac{GH}{2} \cos \theta \right] \end{aligned} \quad (3.6)$$

The moment at the gate pin due to the hydrostatic force is found by applying a moment arm to the differential force in equation (3.1)

$$dM_w = y dF \quad (3.7)$$

Proceeding in a similar manner, the moment at the gate pin for water below the top of the gate is:

$$M_w = \frac{b \gamma h^3}{6 \cos^2 \theta} \quad (3.8)$$

and for water height above the gate the moment is:

$$M_w = b \gamma GH^2 \left[\frac{h}{2} - \frac{GH \cos \theta}{3} \right] \quad (3.9)$$

To account for the velocity head, $h_v = \frac{V^2}{2g}$ equation (3.9) is written:

$$M_w = b \gamma GH^2 \left[\frac{h_{tot}}{2} - \frac{GH \cos \theta}{3} \right]$$

where h_{tot} is the total pressure head at the gate including the velocity head.

$$h_{tot} = h + h_v$$

3.2.2 Ideal Flow Discharge

Assuming a parallel uniform velocity distribution and neglecting effects such as viscosity, surface tension, and gravity, an ideal discharge flow over the gate was found. In the absence of these flow effects, the flow rate over the gate is the theoretical maximum water discharge over the crest of the Flash Gate Board. Applying Bernoulli's equation, the ideal or theoretical flow rate of water over the gate, Q_{theo} , was determined as a function of head above the gate crest and gate angle. Then by measuring the upstream water height, the maximum flow rate for a given gate angle can be calculated.

Neglecting the contraction of the nappe (the free-stream of water over the gate), and the effects of viscosity, a simple equation of discharge can be derived. Figure 5 shows the uncontracted parallel flow over the gate. The nappe streamlines are parallel and atmospheric pressure is assumed throughout. Applying Bernoulli's equation between (1) a distant upstream point on the free surface and (2) at any point above the crest of the gate gives:

$$\frac{V_1^2}{2} + g h = \frac{V_2^2}{2} + g (h - y) \quad (3.10)$$

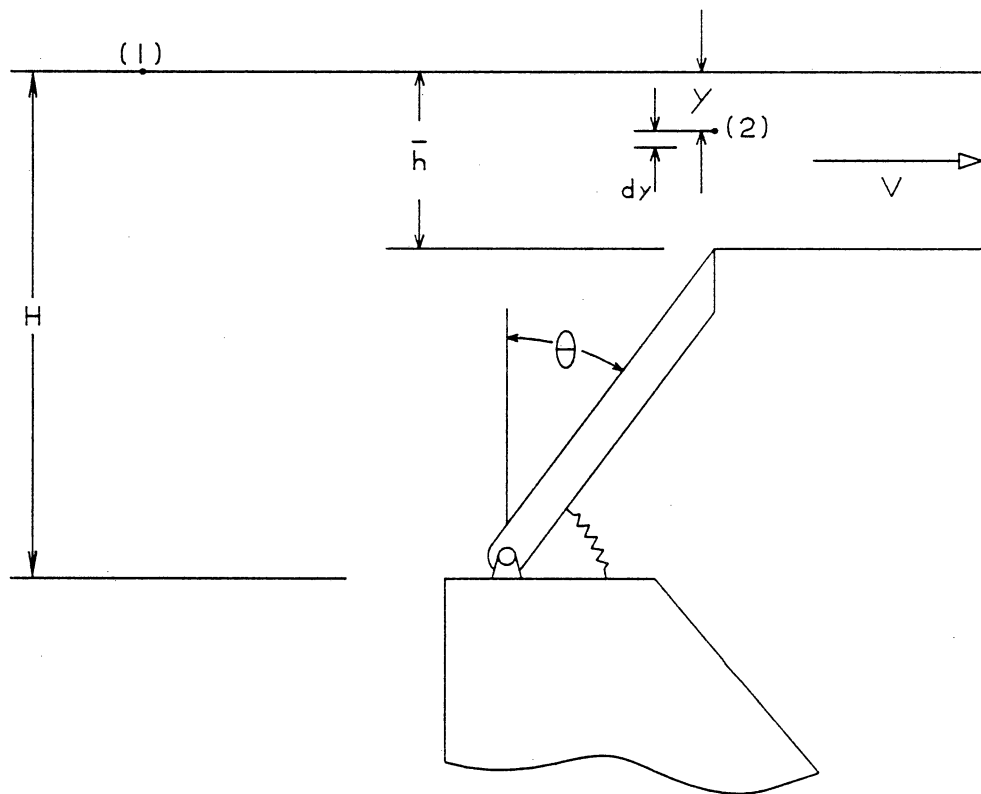


Figure 5. Flash Gate Board with parallel flow

Considering the continuity equation, the velocity of approach, V_1 , is considered negligible compared to the flow velocity over the gate, V_2 . Neglecting V_1 and solving for V_2 gives:

$$V_2 = \sqrt{2gy} \quad (3.11)$$

The theoretical discharge, Q_{theo} , is then found by integrating over the area of the nappe:

$$Q_{theo} = \int_A V dA \quad (3.12)$$

$$\begin{aligned} Q_{theo} &= \int_0^{\bar{h}} \sqrt{2gy} b dy \\ &= \frac{2}{3} b \sqrt{2g\bar{h}^3} \end{aligned} \quad (3.13)$$

where,

$$\bar{h} = h - GH \cos \theta \quad (3.14)$$

Including the head due to the velocity of approach, $h_v = \frac{V_1^2}{2g}$, in the formulation gives a theoretical flow rate of:

$$Q_{theo} = \frac{2}{3} b \sqrt{2g} \left((\bar{h} + h_v)^{3/2} - h_v^{3/2} \right) \quad (3.15)$$

Flow effects cause the actual discharge and moment at the gate pin to be less than the theoretical formulations derived in the preceding two sections. The next section examines these flow effects and provides a means of estimating the actual moment and discharge from the theoretical values.

3.2.3 Actual Moment and Flow Determination

In the preceding sections, equations for the ideal moment and discharge were derived. The following assumptions were necessary for the derivation of these equations:

- negligible flow effects
- parallel streamlines
- uniform upstream velocity distribution
- hydrostatic pressure distribution throughout

The actual moment on the gate and flow over the gate are less than ideal when these assumptions are taken into account. The free-stream of water over the gate, called the nappe, contracts or pulls down because of gravity, surface tension and the radial velocity needed by the fluid to flow over and around the crest and sides of the gate. This contraction of the nappe causes less water to be on the gate at a given time, reducing the effective headwater pressure available to contribute to the hydrostatic moment. A reduction in flow results.

Viscosity, surface tension, and gravity, along with end effects cause streamlines near the crest to be curved. Thus, the assumptions of uniform flow and hydrostatic pressure distributions are poor. To accurately determine the actual moment and discharge requires the use of empirically determined coefficients.

The coefficients are determined by comparing actual moments and flows to theoretical predicted values. The actual moments and flows for fixed gate angles and water heights are obtained through experimentation. The moment coefficient, C_m , and discharge coefficient, C_d , are defined as:

$$C_m = \frac{M_{w_{act}}}{M_{w_{theo}}} \quad (3.16)$$

$$C_d = \frac{Q_{act}}{Q_{theo}}$$

Information on discharge coefficients for weirs at various downstream facing angles can be found in the literature (Chow 1959 [4], Davis 1969 [7], Justin 1928 [5]). These weirs resemble the Flash Gate Board thus making their discharge coefficients useful for determining actual flow rates for the Flash Gate Board. From Bazin's experiments (Chow 1959 [4]), Figure 6, presents these discharge coefficients as a function of gate angle for angles up to 50 degrees. At angles greater than 50 degrees the gate begins to act like a broad-crested weir (see Figure 7). The nappe is fully supported and the flow reaches a critical depth of $y_c = \frac{2}{3} h_{tot}$ at a velocity of $\sqrt{g y_c}$. This effect is not as prominent when properly designed piers and shorter gates are used. Using this information the discharge coefficient for a gate angle of 90 degrees was calculated. The discharge coefficients from 50 to 90 degrees were interpolated, shown dashed in Figure 6. The coefficients in Figure 6 include the constant terms $\frac{2}{3} \sqrt{2g}$ in equation (3.13), therefore the actual flow is:

$$Q_{act} = C_d b \bar{h}^3 \quad (3.17)$$

In order to generalize the results of Figure 6 a fourth degree polynomial curve fit was performed. Table 1 gives the results of this curve fit.

Table 1. Discharge coefficient curve fit results

$$C_m = a_4 \theta^4 + a_3 \theta^3 + a_2 \theta^2 + a_1 \theta + a_0$$

i	a_i
0	0.3034956E 01
1	0.7062721E-01
2	-0.2000673E-02
3	0.2215820E-04
4	-0.9617463E-07

with θ expressed in degrees

Moment coefficients are not discussed in the literature, but experimentally determined weir nappe shapes (Davis 1969 [7]) for various downstream facing weir slopes can be found. These nappe

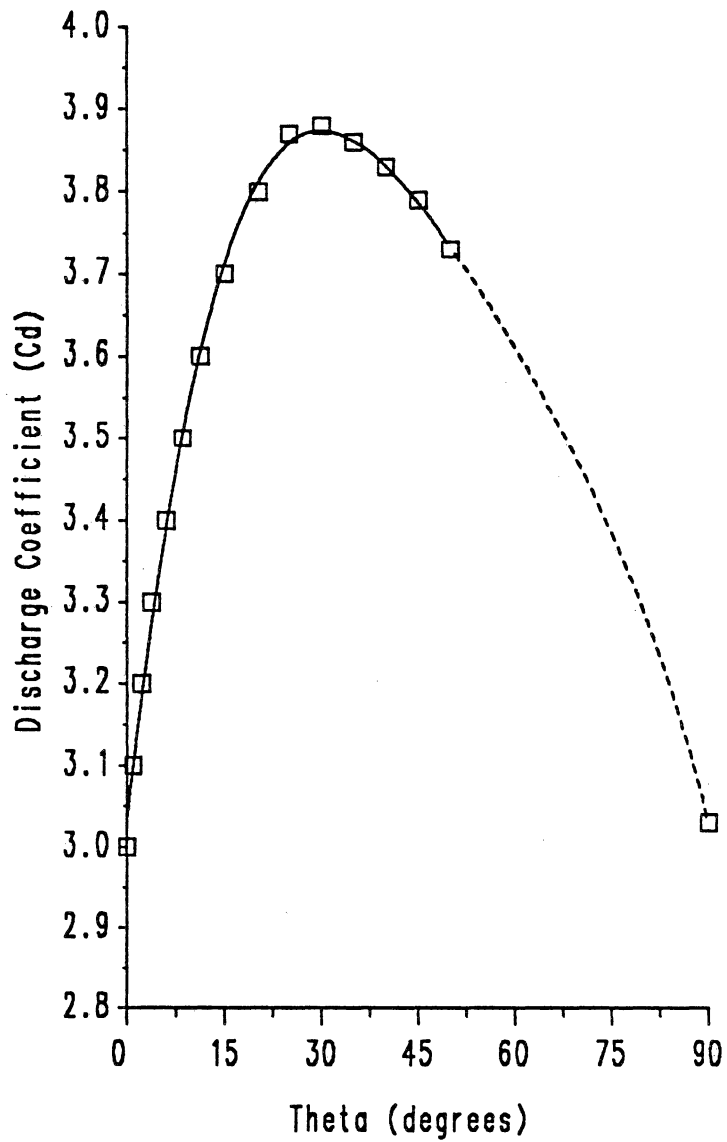


Figure 6. Empirical discharge coefficients

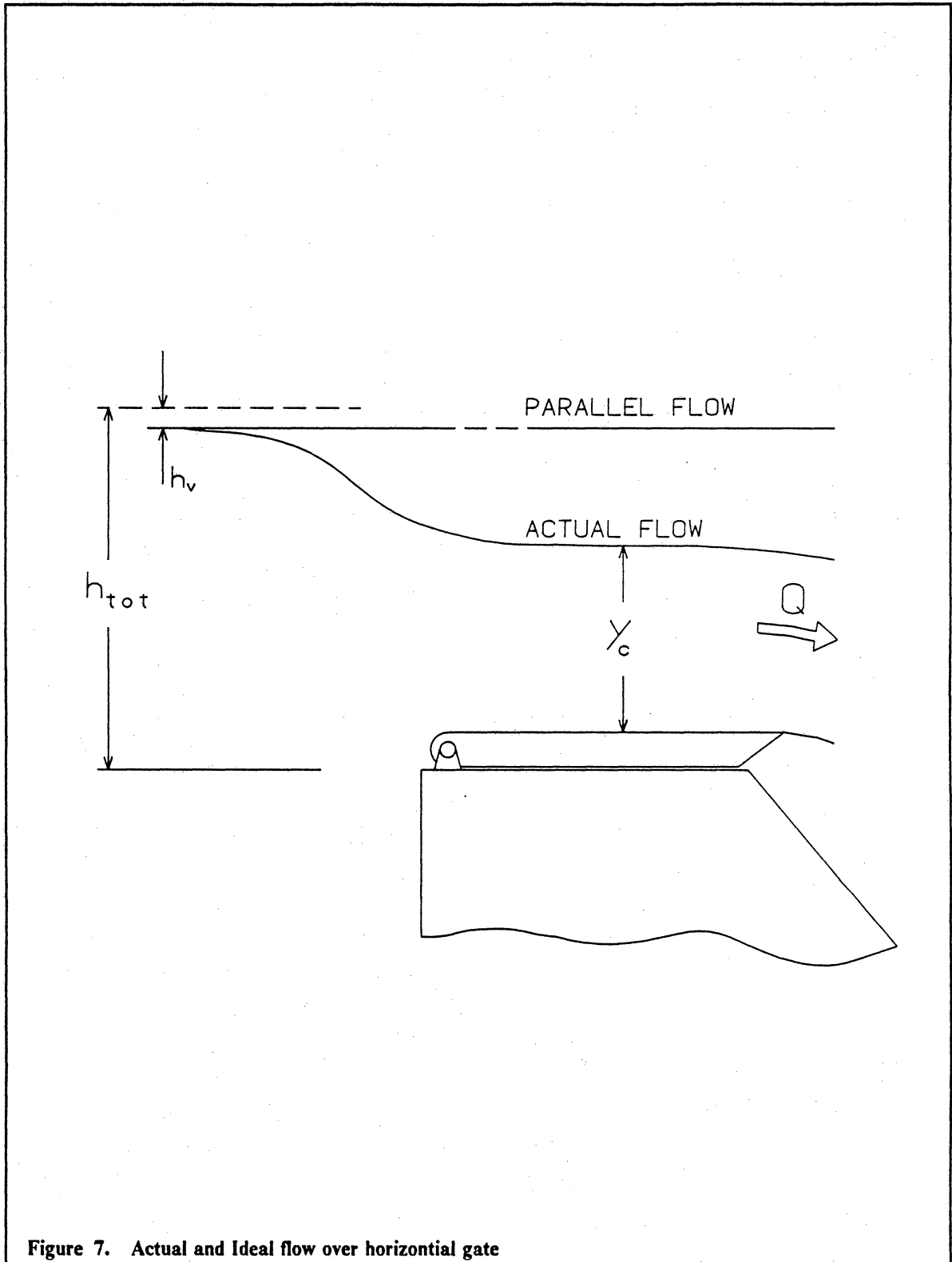


Figure 7. Actual and Ideal flow over horizontal gate

shapes were used to calculate a reduction in flow area from ideal parallel flow due to nappe contraction effects. Knowing the reduction in area a theoretical moment coefficient was calculated as:

$$C_{mc} = \frac{A_{ideal} - A_{contraction}}{A_{ideal}} \quad (3.18)$$

This coefficient is calculated for gate angles up to 60 degrees. Beyond this angle documentation is not available on nappe shapes. At gate angles of 75 and 90 degrees from the vertical, the nappe shape was estimated. Using these estimates the area reductions were found. Equation 3.18 is then used to find the corresponding moment coefficients.

Figure 8 shows the results of using the area reduction method to determine the moment coefficient. The squares present the calculated values and the dashed line represents the results of a third degree polynomial regression fit of that data. Table 2 contains the polynomial coefficients from the curve fit.

Table 2. Moment coefficient curve fit results

$$C_m = a_3 \theta^3 + a_2 \theta^2 + a_1 \theta + a_0$$

<i>i</i>	<i>a_i</i>
0	0.9550985E 00
1	-0.7487063E-03
2	0.4601361E-05
3	-0.1050312E-06

with θ expressed in degrees

Although this method of using area reduction to theoretically determine the moment coefficients provides a way of better estimating the actual flow, the weak assumption of a hydrostatic pressure distribution on the gate still exists. In the experimental section, a method of experimentally determining the actual moment at the gate pin and the results of this experiment are presented.

The previous sections make some assumptions about the flow effects over the gate. Moment and discharge coefficients as a function of gate angle were determined to find the influence of the flow effects with changing gate angle. The severity of the flow effects is also dependant on the geometry

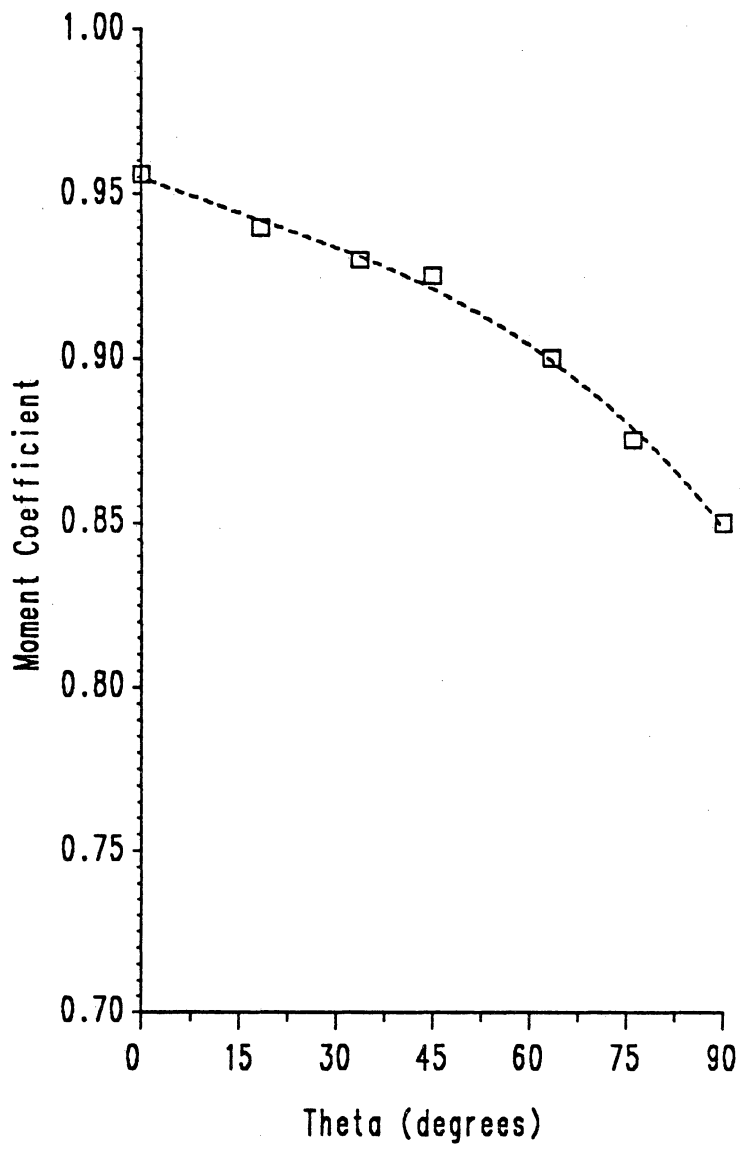


Figure 8. Calculated moment coefficients vs. gate angle

of a specific design along with the design's operational constraints. Examples of some of these determining factors are; gate to dam height ratio, upstream water height, and effective crest length. The effective crest length varies with the type of pier used between gate sections. Piers are needed to form the sides and bearing supports for the gates. Figure 9 shows typical pier shapes and types.

Piers in general cause a flow contraction and in effect reduce the effective length of the spillway crest. The effective length of the spillway crest can be expressed as

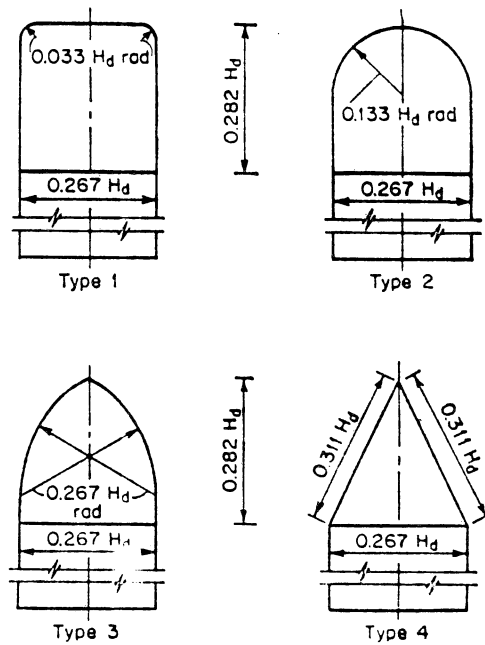
$$L_{eff} = L_o - K n H_{tot} \quad (3.19)$$

where L_o is the spillway crest length before addition of piers and gates; K is the pier contraction coefficient; n is the number of side contractions (2 for each gate section); and H_{tot} is the total head which includes the velocity head. The pier contraction coefficient varies from 0.1 for thick, blunt upstream pier noses to 0.035 for round noses (Chow 1959 [4]). A more detailed look at these effects can be found in (Chow 1959 [4]) and (Creager and Justin 1927 [5]).

3.2.4 Static Results

The static equations are used to develop models to study the static behavior of the Flash Gate Board at various water levels and flow rates. This section presents the results of the static study. The results are used to investigate the restoring spring requirements. Two desired gate angle versus reservoir water height curves (profiles) are hypothesized and the static equations are used to determine the spring torque and variable spring rate required to give the desired angle versus head curve.

Figure 10 is a plot of the theoretical moment versus water height for fixed gate angles. Equations (3.8) and (3.9) were used to develop this plot by holding the gate angle constant and varying the upstream water height from zero to four feet. Each curve represents a fixed gate angle. A gate height of two feet and unit gate width were assumed.



PIER NOSE SHAPES

Note: Pier nose located in same plane as
upstream face of spillway

Copied from (Chow, 1959 [4])

Figure 9. Typical pier types

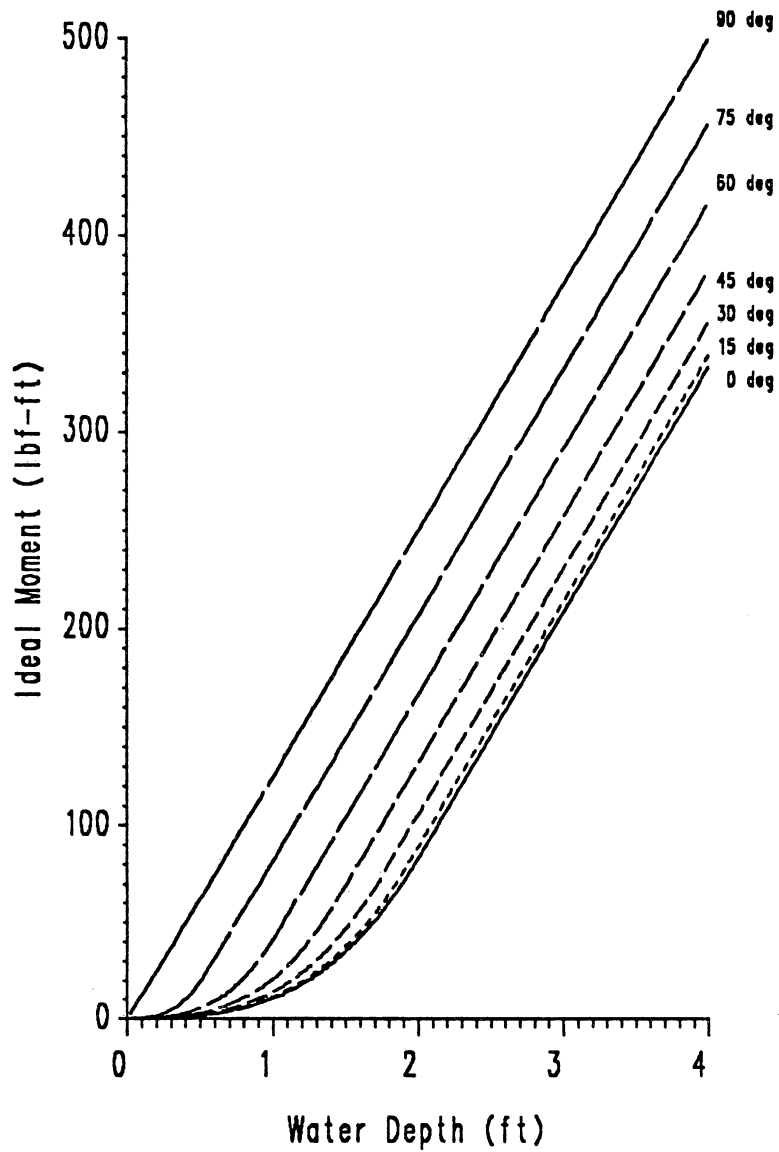


Figure 10. Theoretical moment vs. water height for fixed gate angles

Similarly, equation (3.13) was used to plot the ideal discharge versus water height for fixed gate angles. The results are shown in Figure 11 on page 30. Again, a gate height of two feet and unit width were assumed. Each curve represents a fixed gate angle.

The moment and discharge coefficients discussed in section 3.2.3 were applied and the actual moment and flow versus water height for fixed gate angles are shown in Figure 12 and Figure 13. The coefficients are applied only at flow conditions.

These results were used to investigate the types of restoring spring a typical gate will require. This was done by picking the desired action of the gate for a given water depth (by choosing the gate angle for a given water depth). Then, by equating the spring torque with the water moment, $T_s = M_w$, equations 3.8, 3.9 and 3.16 were used to determine the required spring torque. Differentiating the required spring torque with respect to the gate angle, θ_{gate} , gives the required torsional spring rate as a function of gate angle, θ_{gate} . A FORTRAN program was written to perform these calculations for a given gate angle versus water height curve. The results for two cases are shown in Figure 14 and Figure 15.

Figure 14 shows the result of a linear gate angle versus water depth curve (Figure 14a). Figure 14b and c are the required spring torque and torsional spring rate respectively. Referring to Figure 14c, a spring that softens (provides proportionally less torque with increasing gate angle) with gate angle is required to give the linear gate angle versus water height curve shown in Figure 14a.

The second design gate angle versus water height is a quadratic. This will keep the gate in an upright position longer, constraining more water. Figure 15 shows the results of this design. Referring to Figure 15c, the required spring is hardening at small gate angles and then softens as the gate approaches the vertical position. However, Figure 15b, the required spring torque, resembles a straight line indicating a linear spring may give a gate angle versus water depth curve that approximates the quadratic curve.

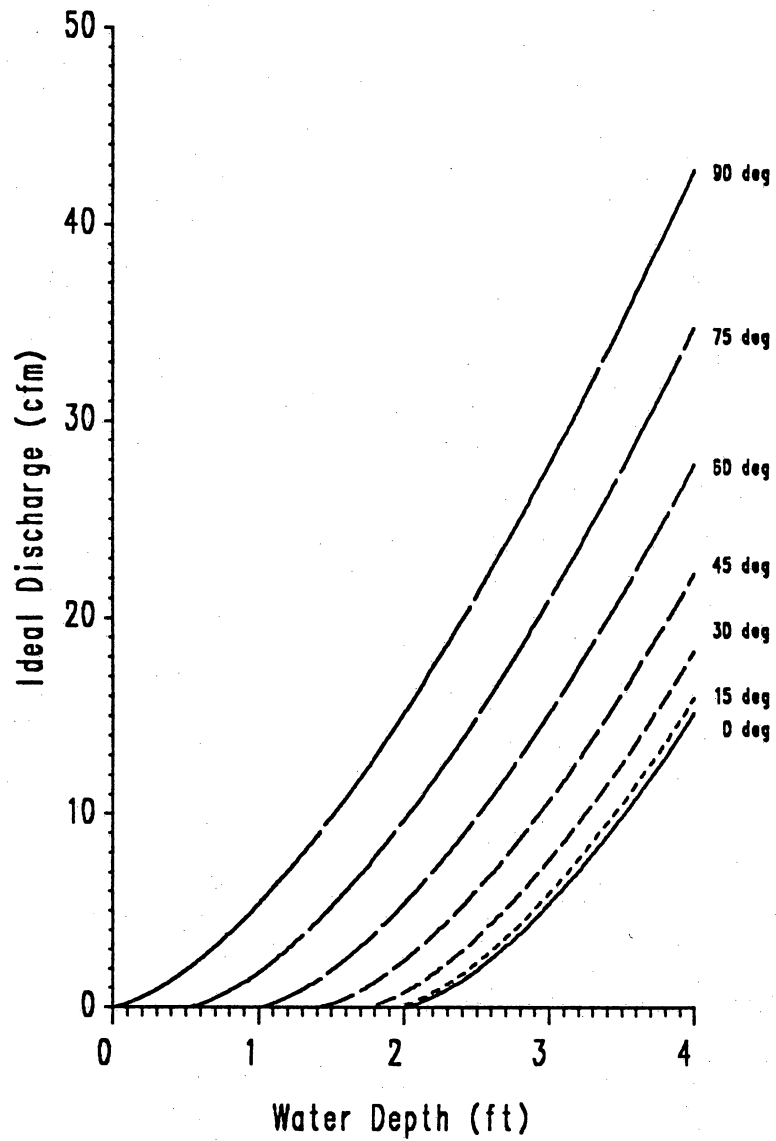


Figure 11. Theoretical discharge vs. water height for fixed gate angles

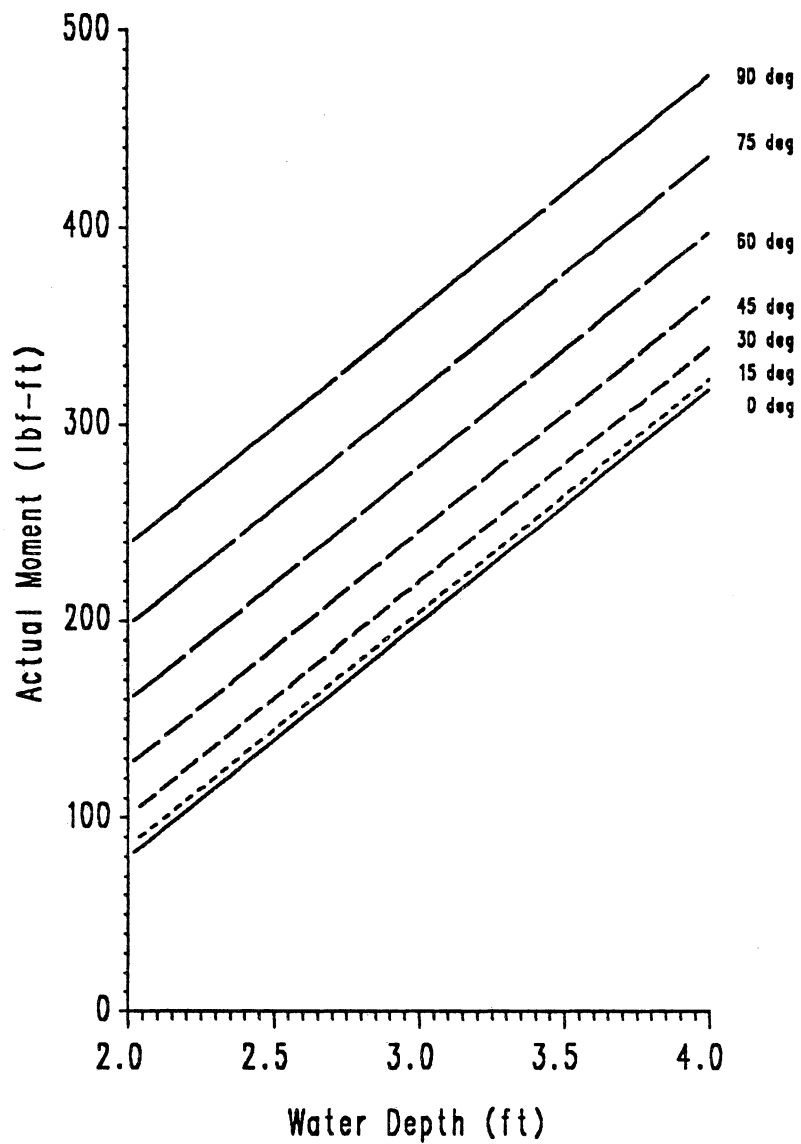


Figure 12. Actual moment vs. water height for fixed gate angles

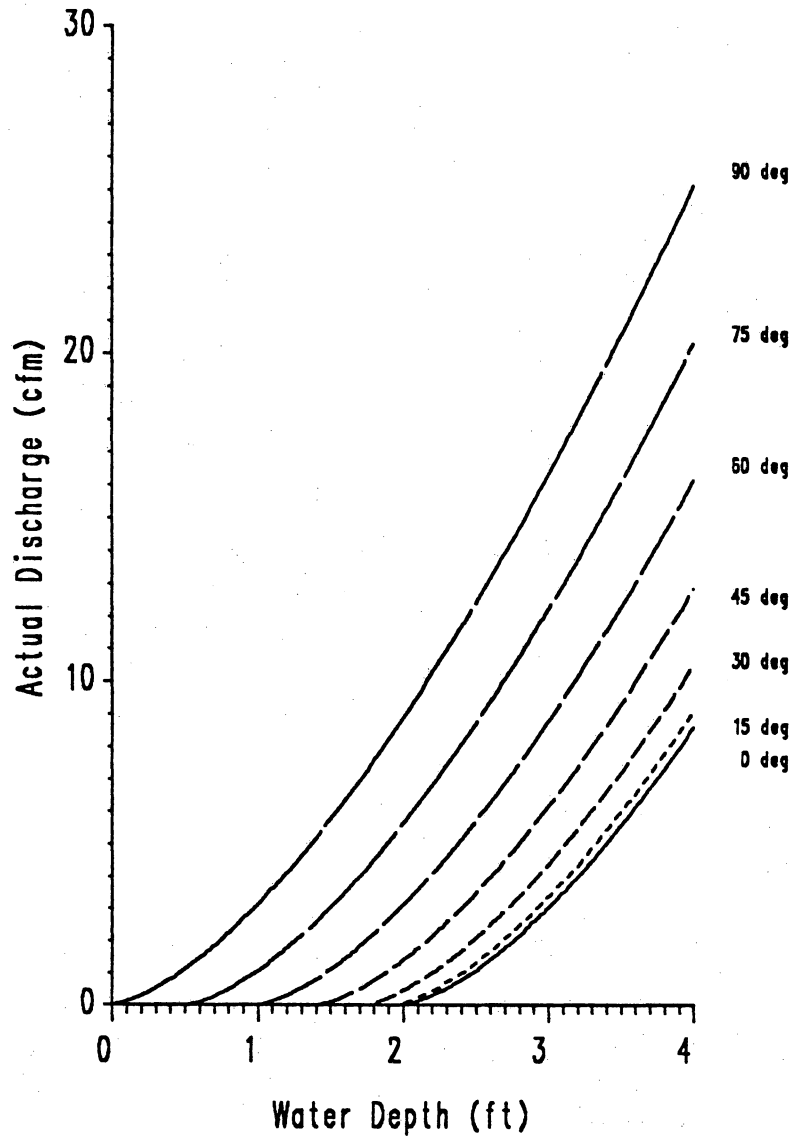
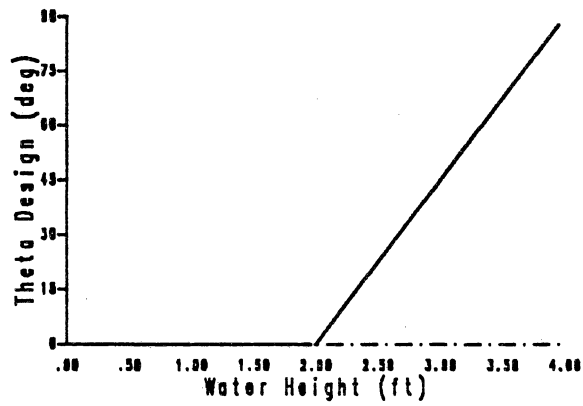
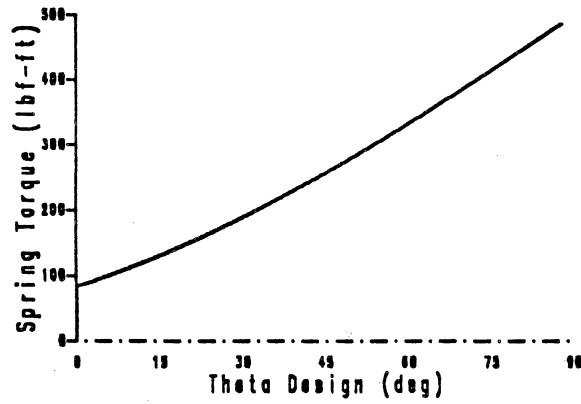


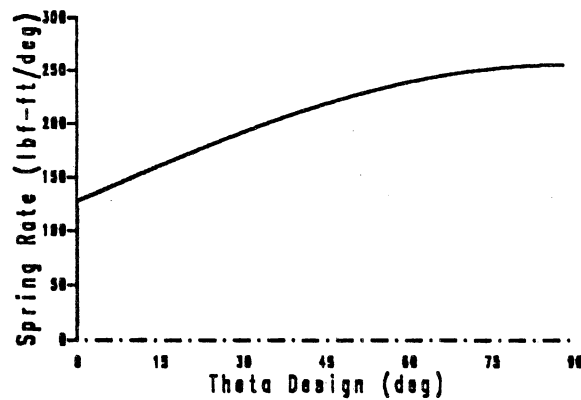
Figure 13. Actual discharge vs. water height for fixed gate angles



(a) Theta design vs. Water height

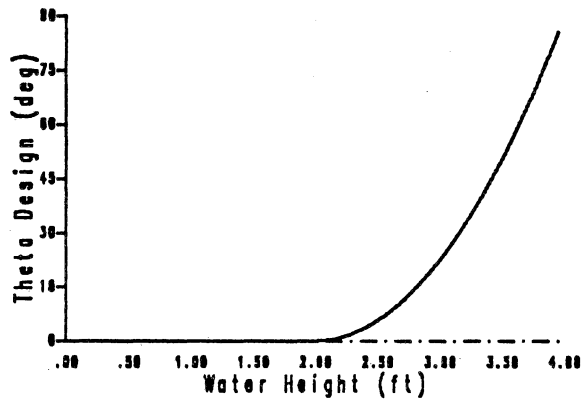


(b) Required spring torque vs. theta design

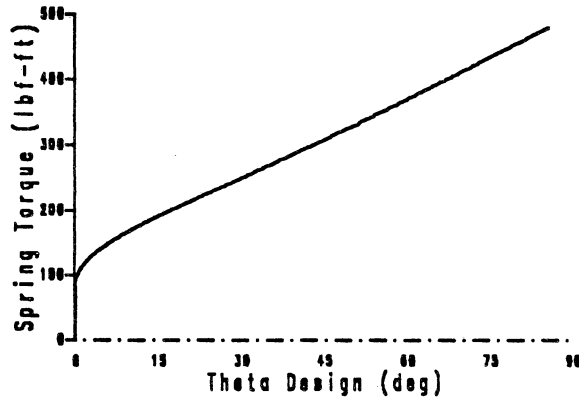


(c) Spring rate to give required torque

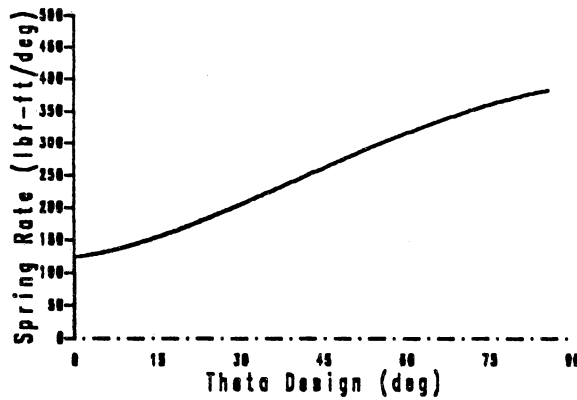
Figure 14. Results of linear theta design vs. water height



(a) Theta design vs. water height



(b) Required spring torque vs. theta design



(c) Spring rate to give required torque

Figure 15. Results of quadratic theta design vs. water height

The program used to obtain Figure 14 and Figure 15 was modified to give gate angle versus water depth for five linear spring rates. The five constant spring rates were chosen based on the above results. The results are shown in Figure 16. These results were found assuming a two foot gate with unit gate width. Each spring was given the same preload, which was set equal to the torque required to keep a two foot gate vertical until the water depth exceeds the gate height of two feet. As expected, the results resemble the quadratic design curve. The linear spring gives an acceptable static performance, and due to its simplicity compared to a non-linear spring, a linear torsion spring was chosen to provide the restoring spring torque.

Two types of linear torsion spring designs were investigated; (1) a torsion bar spring, and (2) a helical torsion spring. The next section provides an overview of the design of these two springs.

3.2.5 Spring Design

This section outlines the basic design process for two types of linear torsional restoring springs; (1) a torsion bar spring and (2) a helical torsion spring. For a linear spring, the spring rate required by the Flash Gate Board is the slope of the torque versus gate angle curve which is the difference between the required torque at the horizontal position and the required torque at the initial (vertical) gate angle divided by the difference in the horizontal gate angle and initial gate angle.

$$K_t = \frac{T_{horiz.} - T_{initial}}{\theta_{horiz.} - \theta_{initial}} \quad (3.20)$$

This spring rate is the same for both types of springs mentioned above. The spring must also include a preload torque equal to the initial required torque to maintain the gate at its prescribed position during normal conditions.

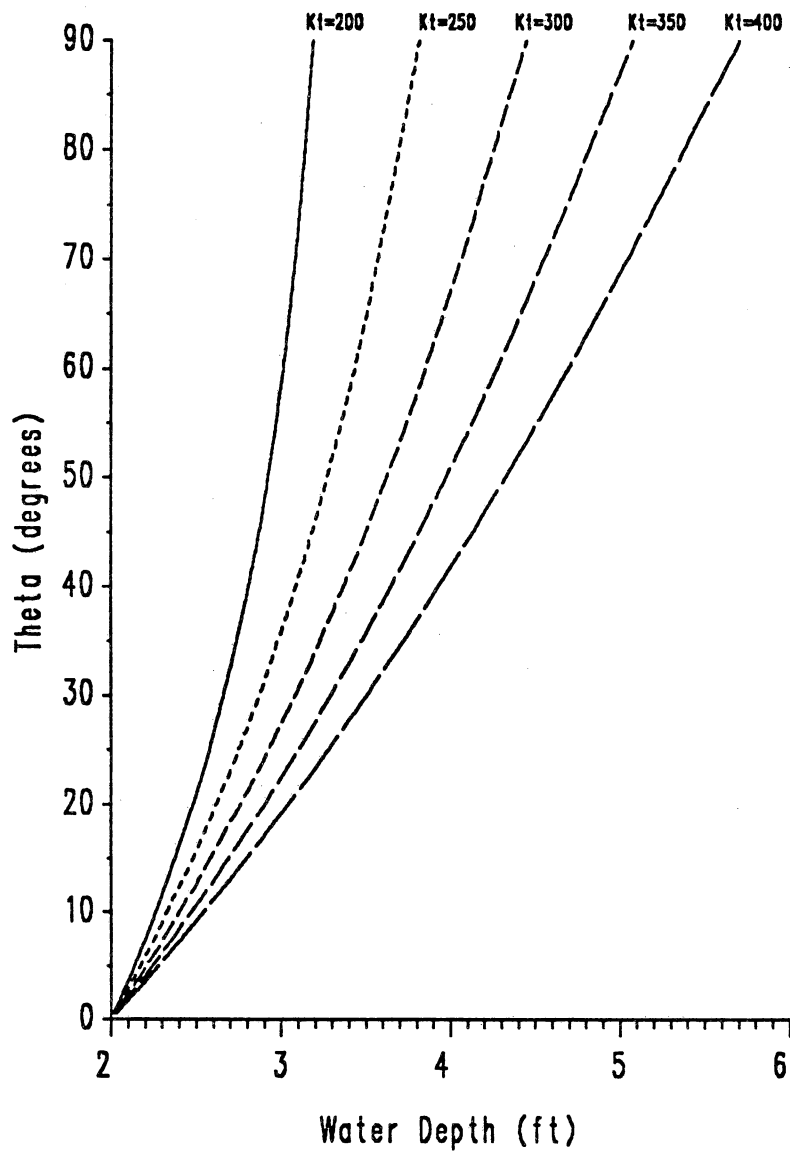


Figure 16. Gate angle vs. water height for linear springs

3.2.5.1 Torsion Bar Spring

A standard torsion bar spring is shown in Figure 17 on page 38. The torsion bar spring is a solid or hollow bar with one end attached to the gate and the other end fixed. The torsion bar spring is appealing as a restoring spring for the Flash Gate Board because of its simplistic design and its potential for easy installation.

Assume a solid bar length, l , diameter, d , supported so that bending effects are negligible, the torsional spring rate is:

$$K_t = \frac{\pi d^4 G}{32 l} \quad (3.21)$$

Where G is the torsional modulus of elasticity of the torsion bar material.

To certify the torsion bar as a valid solution to the restoring spring problem, a stress analysis, checking for both static and fatigue failure, was performed on six different torsion bar spring and gate configurations. Table 3 summarizes the results of this analysis. In case (i) the gate is held vertical until the water depth exceeds the gate height. A two foot gate and four foot flood rights were assumed. In case (ii) the gate is held at 30° from the vertical until the water depth reaches 2.5 feet. A gate length of 2.3 feet and flood rights of four feet were used. This case is consistent with the inventors original design ideas (Johnson 1980 [10]). In both cases a factor of safety of one is used and bending moment effects are not considered.

Table 3. Results of torsion bar stress analysis

case	gate length	configuration	result
i	8 ft	2-4 ft bars	static failure indicated
i	8 ft	1-8 ft bar	static failure indicated
i	8 ft	2-8 ft bars	fatigue failure indicated
i	10 ft	2-10 ft bars	fatigue failure indicated
ii	8 ft	1-8 ft bar	static failure indicated
ii	8 ft	2-8 ft bars	just within safe limits

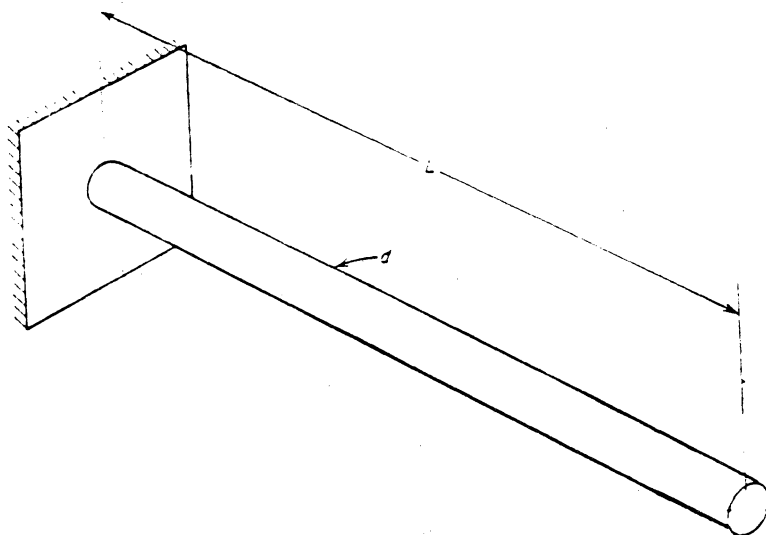


Figure 17. Typical torsion bar spring

As indicated in Table 3, static failure was indicated in three of the six cases and fatigue failure was indicated in two of the remaining three cases. The one case where neither static or fatigue failure was indicated was just within the limits of an acceptable design with a factor of safety of only one. Based on these results, the torsion bar was discarded as a possible choice for the restoring spring.

3.2.5.2 Helical Torsion Spring

A helical torsion spring deflects through an angle about its coiled axis. Figure 18 illustrates a helical torsion spring with a round cross section. The torsion bar spring design has only two design parameters; wire diameter d , and wire length l . The helical torsion spring gives the spring designer three parameters to select; wire diameter d , mean spring diameter D , and number of coils N (see Figure 18), offering the designer greater flexibility.

The following equations and guidelines are presented as a procedure for designing an acceptable helical torsion spring from round wire. The spring rate is:

$$K_t = \frac{d^4 E}{67.9 D N} \quad (3.22)$$

Where the 67.9 term is from the moment of inertia calculation with an experimental correction factor applied (Shigley, 1983 [24]). E is the modulus of elasticity of the spring material. The spring index, C is defined as:

$$C = \frac{D}{d} \quad (3.23)$$

for a good design the range of the spring index should be: $4 < C < 14$. The total number of coils should be: $3 < N < 30$. For $N < 3$ the spring will buckle easily and for $N > 30$ the spring will not deflect simultaneously. The free length of the spring is found from,

$$L = N(d + s) \quad (3.24)$$

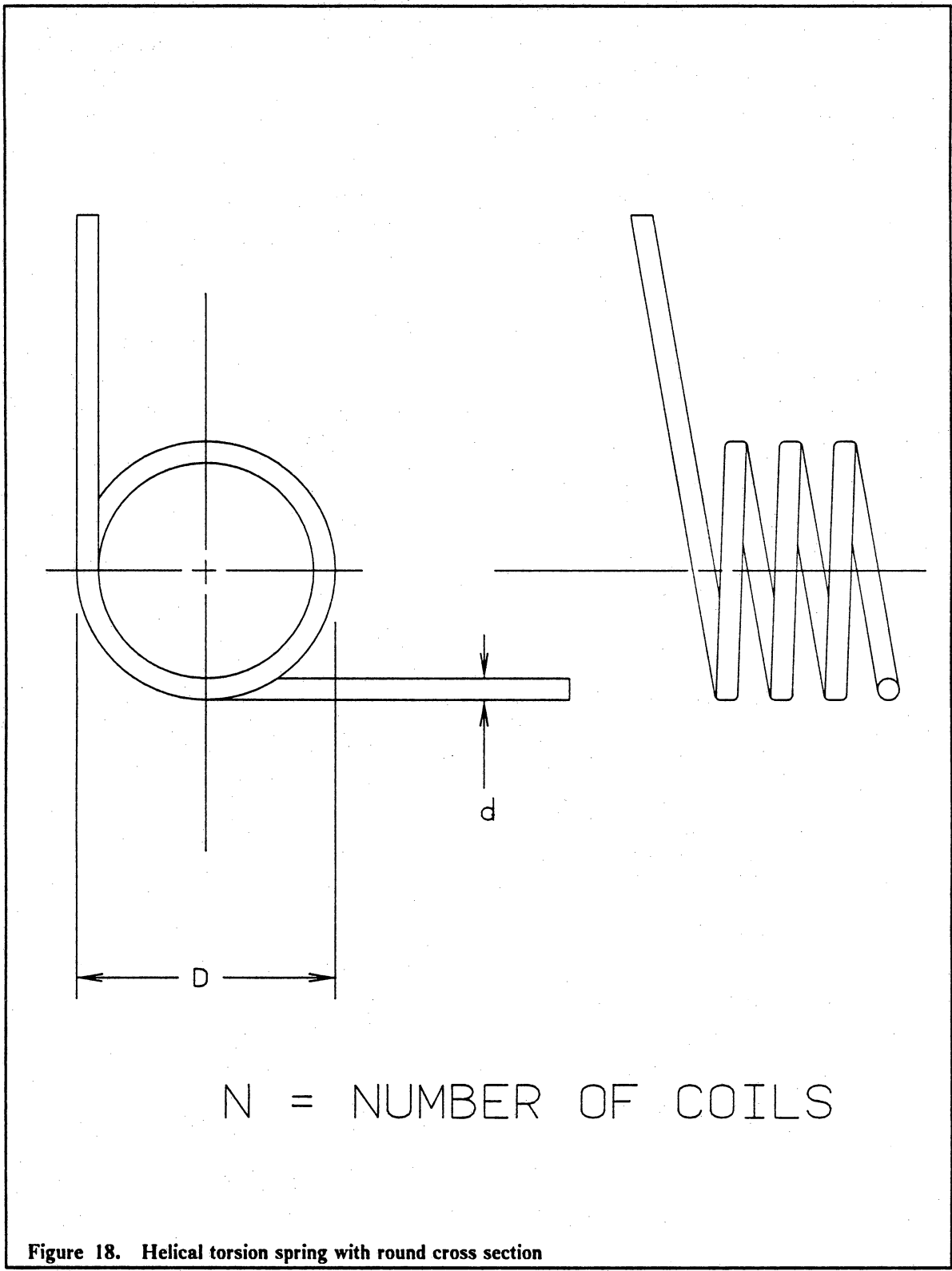


Figure 18. Helical torsion spring with round cross section

where s is the spacing between coils. The spacing between coils should be at least 20 percent of the wire diameter, d . It is also important to insure the loaded inside diameter does not bind on the gate pin or a bending failure will occur. When the spring deflects its inside diameter reduces according to;

$$D'_i = \frac{N}{N'} D_i \quad (3.25)$$

Where D'_i is the loaded inside diameter, N' is the loaded number of coils, D is the unloaded inside diameter, and N is the unloaded number of coils.

The helical torsion spring design process is a recursive trial and error process. A helical torsion spring design software package was developed to aid in the spring design process. The spring design software and a user's guide are available from the VPI & SU Mechanical Engineering Department.

3.3 Dynamic Analysis

The preceding sections analyzed the static or steady state behavior of the Flash Gate Board. Based on the static results it appears the Flash Gate Board is a feasible means of extending the spillway height of an overflow dam. This section expands on the static work of the the last section and addresses the question of dynamic feasibility. To be dynamically feasible the Flash Gate Board must be stable under normal conditions (*i.e.* no self-excited vibrations) and all transients from disturbances (due to wave or debris impact) must decay in a reasonable time.

A dynamic model of the Flash Gate Board was developed and used to study the transient behavior of the Flash Gate Board system. The model was developed by deriving the governing differential equations of the system. The development of these equations is presented along with the results of the dynamics study. Two dynamic models were developed; (1) a fast model, to investigate the

gate response to impulsive forces such as debris impact and (2) a slow model, which was used to study the gate behavior under various rain conditions.

The fast model includes the dynamics of the gate and the dynamics of the reservoir. Differential equations describe the motion of the gate and the reservoir height. The slow model includes only the reservoir dynamics. Only the reservoir height is described in differential form; the gate position is statically defined by a set of algebraic equations. The slow model is justified because the time constant of the reservoir is several orders of magnitude slower than the period of the gate motion. Describing the gate statically allows for a larger time step in the simulation and thus longer simulations can be run economically. Long simulations are necessary to study the system's behavior for extended periods (days) of rain.

The derivation of the dynamic model begins with the rotational equation of motion (EOM) for the gate. Each term in the equation is subsequently explained and derived in the sections that follow. Next, the rotational EOM is coupled with the EOM for the reservoir height. Finally, the results of using these equations to build a dynamic simulation model are presented. Included in these results is an investigation into the possibility of an optimum gate height for a given reservoir.

3.3.1 Rotational Equation of Motion

The rotational EOM for the Flash Gate Board system is found by applying Newton's second law. For rotation the law stated in equation form is:

$$\Sigma M = J \alpha \quad (3.26)$$

where ΣM is the sum of the moments acting on the body, J is the system's total moment of inertia about the axis of rotation, and α is the angular acceleration of the body about the axis of rotation.

Referring to the freebody diagram shown in Figure 19, the equation of motion of the Flash Gate Board system is:

$$J_v \ddot{\theta} + C \dot{\theta} + K \theta = M_w + M_d \quad (3.27)$$

J_v is the system's total moment of inertia (or virtual inertia) including the added inertia of the water, C is the viscous damping coefficient, and K is the torsional spring rate. M_w is the moment due to the headwater pressure and M_d is a moment due to hydrodynamic drag. In the following sections the derivation of each of these is presented.

3.3.1.1 *Virtual Inertia*

The virtual or "effective" moment of inertia of the gate comes from the combined effects of the actual moment of inertia, due to the mass of the gate, and the added inertia caused by the surrounding fluid. The added (also called attached) mass that contributes to the virtual inertia of the gate can be defined as the mass that must be added to the gate in the absence of fluid to reproduce the total force acting on the gate due to the fluid presence.

There are several computation techniques available for computing the added mass of a body vibrating in a fluid. Some of these methods for a body in harmonic vibration are:

- conformal mapping
- three dimensional linear wave theory
 - boundary integral method
 - finite element method
- experimental electrical analogy (see Zienkiewics 1969 [26])

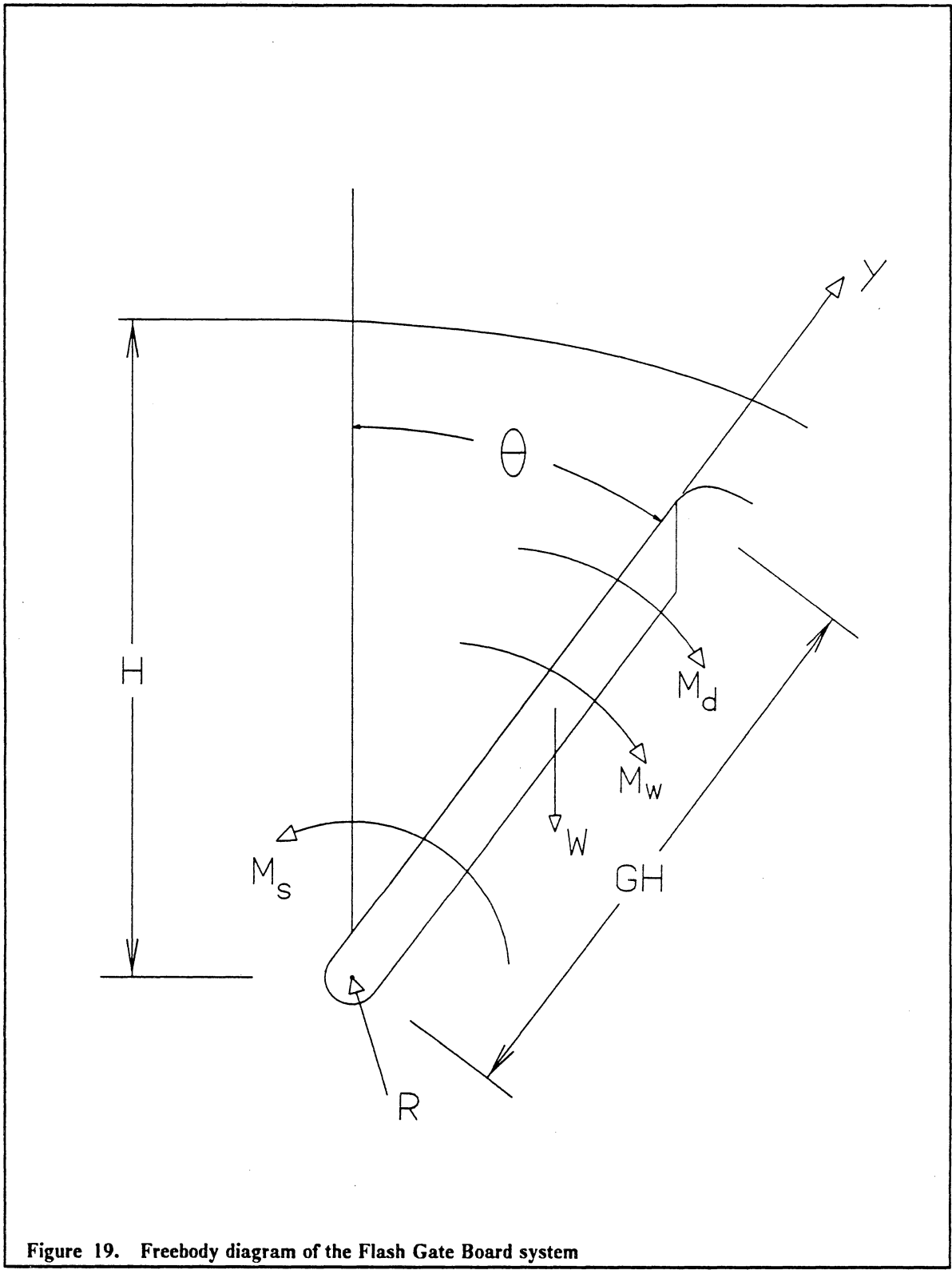


Figure 19. Freebody diagram of the Flash Gate Board system

All of these methods assume small amplitude harmonic motion of the body. Stagnant fluid with an induced potential flow field is also assumed. Small amplitude vibration must be assumed because the vibrating body is replaced with a stationary body with a potential source distribution. The source is such that its discharge equals the quantity of water displaced by the vibrating body. (Novak 1984 [14])

The added mass is affected by the flow velocity, the frequency of gate oscillation, and the gate position. Because these parameters are not constant in the Flash Gate Board system, an estimate of the added moment of inertia as a function of gate angle and gate length was made. For this study the added inertia was taken to be equal to the mass of the quantity of water swept out by the arc of the gate. This model for the added inertia gives a lower total inertia than other models and results in a higher natural frequency of the gate system. Figure 20 shows the added inertia estimate for a general gate position. The virtual moment of inertia is then:

$$J_v = J + J_a$$

where J is the moment of inertia due to the mass of the gate and J_a is the added inertia of the surrounding fluid, or

$$J = \frac{1}{3} m GH^2$$

$$J_a = \frac{b \gamma GH^4 \theta}{2g}$$

3.3.1.2 Linear Spring

The linear spring rate, K , provides a restoring moment to the gate proportional to the gate angle.

$$M_s = K [\theta + \theta_{preload}] \quad (3.28)$$

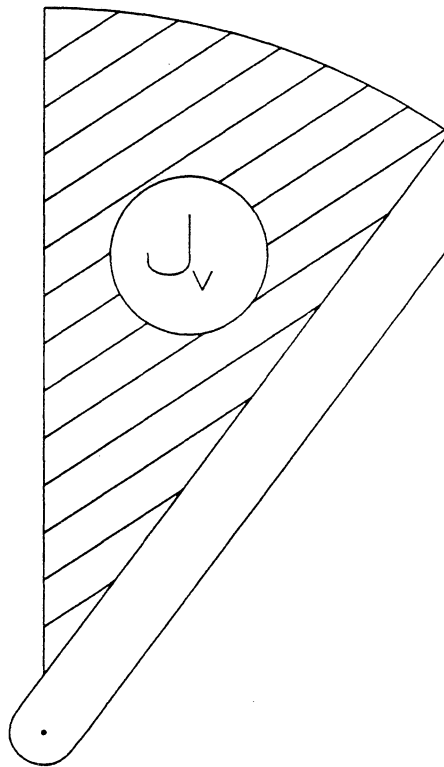


Figure 20. Added inertia for general gate position

Where θ is the gate angle and $\theta_{preload}$ is the required preload angle of the spring. The spring rate, K , was chosen according to the criteria outlined in section 3.2.4. The preload moment, $K \theta_{preload}$, was set equal to the torque necessary to keep the gate upright at water heights less than the gate height. The spring torque at $\theta = 90^\circ$ was set equal to the water moment at the gate's full open position with the water depth at the corresponding activation height (assumed to be flood rights). Using equation (3.20) K was determined as a function of gate height, gate length, and water activation height. Assuming the gate remains vertical ($\theta = 0^\circ$) until the water depth exceeds the gate height, K is:

$$K = \frac{b \gamma GH^2}{\pi} \left(FR - \frac{1}{3} GH \right) \quad (3.29)$$

Equation (3.29) assumes the gate is not fully open until the water reaches the flood rights level. If it is desired to have the gate fully open at some water level lower than flood rights, this value can be directly substituted for FR in equation (3.29). The derivation of this equation also assumes the gate initially remains vertical until the water level exceeds the gate height. If a different initial condition is desired, equation (3.20) can be used to determine the required spring rate.

3.3.1.3 Headwater Moment

The moment due to the headwater pressure is found by applying the moment coefficient, defined in Table 2 on page 24, to equation (3.9), the theoretical headwater moment.

$$M_w = C_m(\theta) M_{w,theo}(\theta, h, GH, b) \quad (3.30)$$

Equation (3.8) is used when the water depth is below the gate height.

3.3.1.4 Viscous Damping Coefficient

The damping term, $C\dot{\theta}$ in equation (3.27) is a measure of the energy dissipated by viscous drag. The viscous damping force is proportional to the angular velocity of the gate. Friction at the gate bearing and gate seal cause viscous drag. The selection of a viscous damping coefficient for use in the model depends on the gate size and the types of bearing and seals used.

A datum for the amount of energy dissipation (damping) is the damping ratio ζ . The damping ratio is the ratio of the system's damping coefficient to the coefficient for critically damped motion.

$$\zeta = \frac{C}{C_{crit}}$$

Critically damped motion is the limiting case between oscillatory and non-oscillatory motion. Therefore, the higher the damping ratio the less the gate will vibrate. Most actual physical systems have damping ratios greater than 0.5. It is believed the Flash Gate Board system will fall into this category. However, to investigate the worst case, a low damping ratio ($\zeta = 0.1$) was assumed in the model. Several higher damping ratios were also checked.

3.3.1.5 Hydrodynamic Damping

The dominant cause of hydrodynamic damping occurs when energy is dissipated in the form of a drag force. As the Flash Gate Board vibrates in the overflowing fluid, its motion is retarded by fluid drag. The drag force acts in line with the relative flow velocity and opposes the motion of the gate. One method for describing the hydrodynamic drag force is:

$$|F_d| = \frac{1}{2} \rho V_{rel}^2 D C_{drag} \quad (3.31)$$

Where V_{rel} is the relative velocity between the fluid and the gate, D is the projected frontal area of the gate, and C_{drag} is an empirical drag coefficient.

The average velocity of the gate is approximately half the gate height times the angular velocity of the gate.

$$\bar{V}_{gate} \approx \frac{GH}{2} \dot{\theta}$$

The average velocity of the fluid is computed by dividing the flow rate over the gate by the upstream area $b h$

$$V \approx \frac{Q}{b h}$$

The relative velocity between the fluid and the gate is then:

$$V_{rel} = (V - \bar{V}_{gate})$$

The projected upstream area of the Flash Gate Board is:

$$D = GH \cos \theta$$

To compute the moment at the gate pin caused by the hydrodynamic drag force, a moment arm of half the projected frontal height is used. The hydrodynamic drag moment, M_d is then:

$$M_d = \frac{C_{drag} \rho L D^2}{4} (V - \bar{V}_{gate})^2 \quad (3.32)$$

The drag coefficient was found for $\theta = 0^\circ$ and $\theta = 90^\circ$ and a linear fit was assumed for all intermediate gate angles. The results of the linear fit are,

$$C_{drag} = 0.732 \theta + 1.2$$

with θ expressed in radians.

3.3.2 Reservoir Dynamics

The equation of motion of the reservoir is determined by applying the continuity equation which states; the time rate of change of the reservoir volume is equal to the volumetric flow input less the volumetric flow output. In equation form, the continuity equation is written:

$$\frac{dV}{dt} = Q_{in} - Q_{out} \quad (3.33)$$

The volume of the reservoir is the reservoir area times the reservoir height. The flow input is due to rain plus drainage. The flow output is the flow over the Flash Gate Board which is a function of gate angle, gate length, gate height, and reservoir water height. Substituting, equation (3.33) is now written:

$$\frac{d}{dt} Ah = Q_{in} - Q_{out}(\theta, h, b, GH) \quad (3.34)$$

Making the assumption of constant reservoir area and uniform reservoir height, equation (3.34) becomes:

$$A \frac{dh}{dt} = Q_{in} - Q_{out}(\theta, h, b, GH)$$

or

$$\dot{h} = \frac{1}{A} (Q_{in} - Q_{out}(\theta, h, b, GH)) \quad (3.35)$$

Q_{out} is determined using equations (3.13) and (3.14) with the discharge coefficients given in Table 1 on page 21. Q_{in} is chosen to be representative of the total inflow (including drainage) to the reservoir for a given rain.

Equations (3.27) and (3.35) were used to build a dynamic simulation model of the Flash Gate Board. This is the fast model that is used to study the transient gate behavior. It is a third order model with two degrees of freedom. The model also includes provisions for analyzing the gate when it slams open or shut. The action of the gate hitting the stops is modeled with an equivalent wall stiffness that increases proportionally with displacement into the wall. Figure 21 is a block diagram of the dynamic model.

The assumptions made in deriving the equation of motion of the Flash Gate Board system were; constant reservoir area, uniform velocity profile, uniform water level in reservoir, and a ventilated nappe. The ventilated nappe assumption is important because trapped air under the nappe acts as an air spring inducing self-excited vibrations. If a specific installation does not allow for natural ventilation of the nappe, artificial means of ventilating must be provided. Some methods of providing nappe ventilation are discussed in chapter 5.

Equation (3.35) and the static gate equations (3.8) and (3.9) are used to build the slow first order simulation model. Equations (3.28) and (3.30) are equated and a fixed point iteration is used to determine the gate angle for a given water depth.

3.4 Dynamic Results

3.4.1 Fast Model

The block diagram of Figure 21 was used to develop a computer simulation of the Flash Gate Board system. This model was used to study the transient response of the gate to various impacts. Mitchell and Gauthier Associates' Advanced Continuous Simulation Language (ACSL) was used

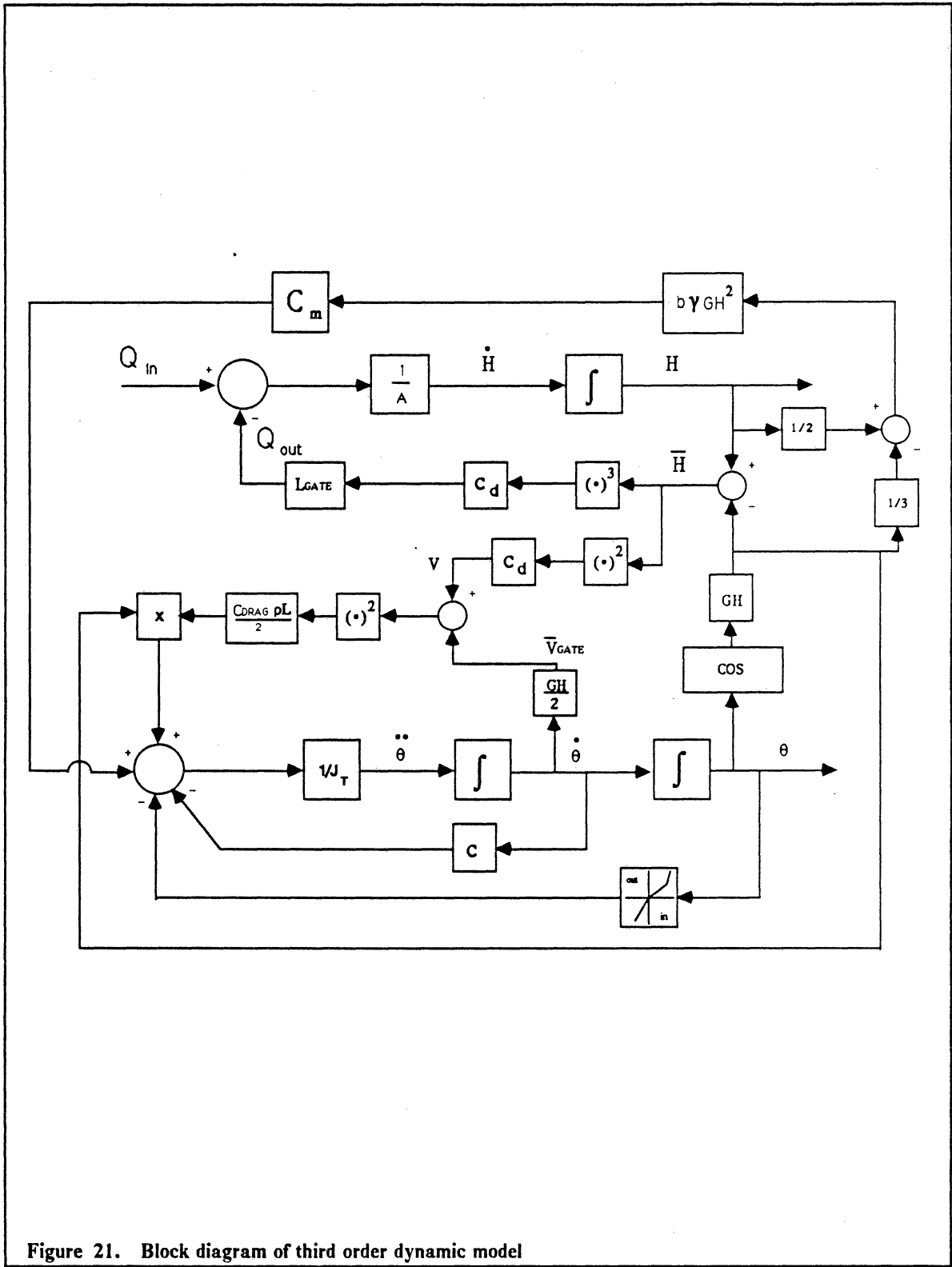


Figure 21. Block diagram of third order dynamic model

to perform the simulations. A wide variety of impacts was investigated with several different sets of initial conditions. This section presents a sample of typical results obtained from simulations using the third order model. An impulse equivalent to the impact of a 20 foot telephone pole on the gate traveling at one mile per hour was used to obtain the sample results. The impulse imparted on the gate was determined through conservation of momentum. The following results were found assuming a two foot gate of unit length, a flood rights level of four feet, and a lake area of one quarter acre. Figures are presented which show:

1. gate and water height response following impact
2. the effects of the dominant terms in the rotational equation of motion.
3. comparative effects of different initial water heights on gate response.

Figure 22 presents the response of the gate angle and the reservoir water height with the third order model following the simulated log impact. From top to bottom, Figure 22 shows: the impulse input that simulates the log impact; the gate angle time response; the reservoir water height time response; and the flow over the gate. An initial water height of 2.5 feet was assumed along with a constant flow input of 0.3 cubic feet per minute. As mentioned above the damping ratio was assumed to be 0.1. Referring to the gate response, all transients die out in approximately three seconds even with the low ($\zeta = 0.1$) damping ratio.

The contribution of each term in equation (3.27) is shown in Figure 23. The input (log impact) is shown at the top of Figure 23 followed by the gate response and the water, spring, and drag moment respectively. It should be noted that the hydrodynamic drag moment is $\approx 180^\circ$ out of phase from the water and spring moments. This produces a stabilizing effect on the gate.

To demonstrate the comparative effects of initial water heights on the gate response, Figure 24 presents three different initial water heights and corresponding gate angles. Each model is the same; only the initial conditions are different. The same impulse is given to each case. From top to

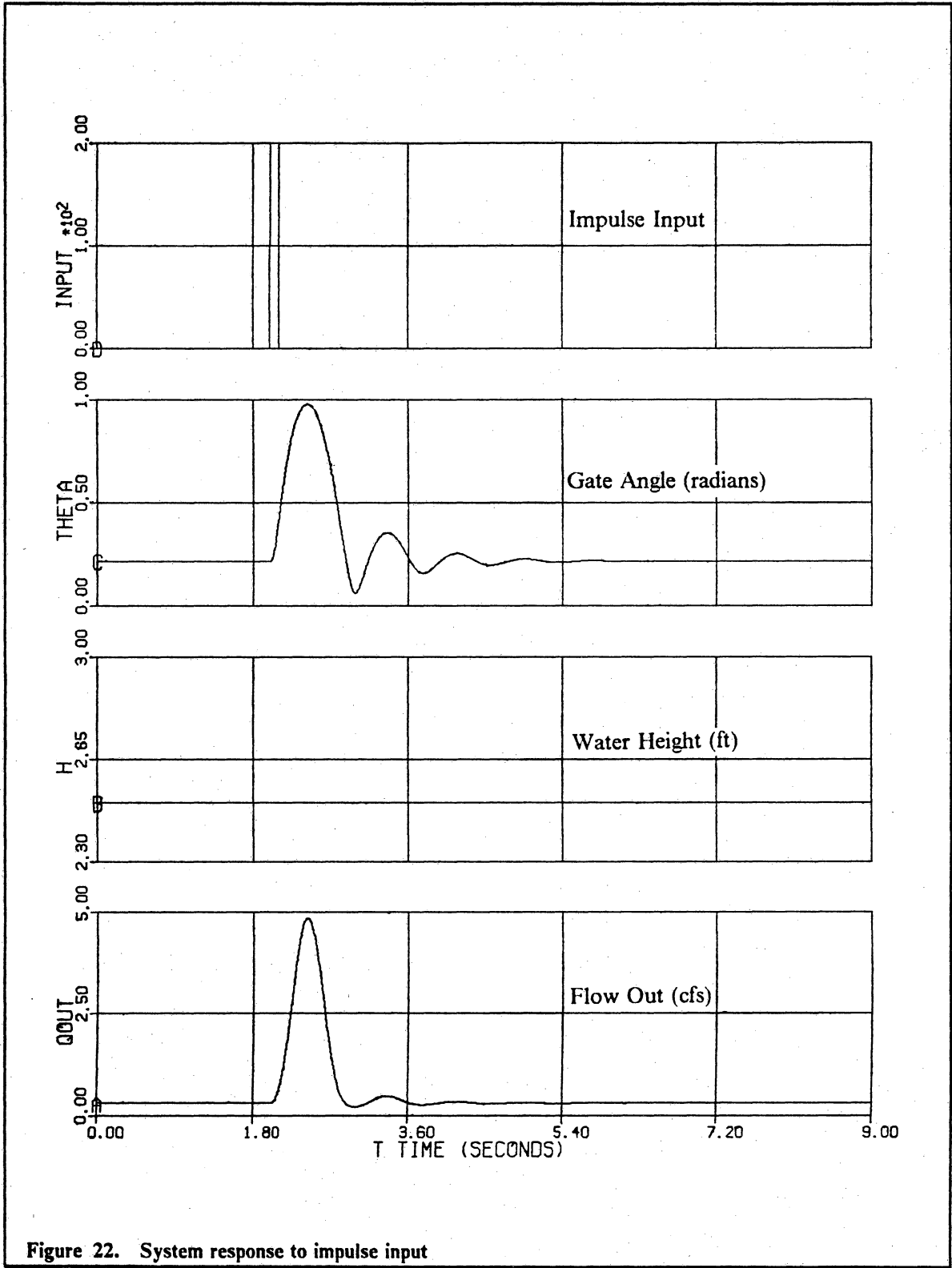


Figure 22. System response to impulse input

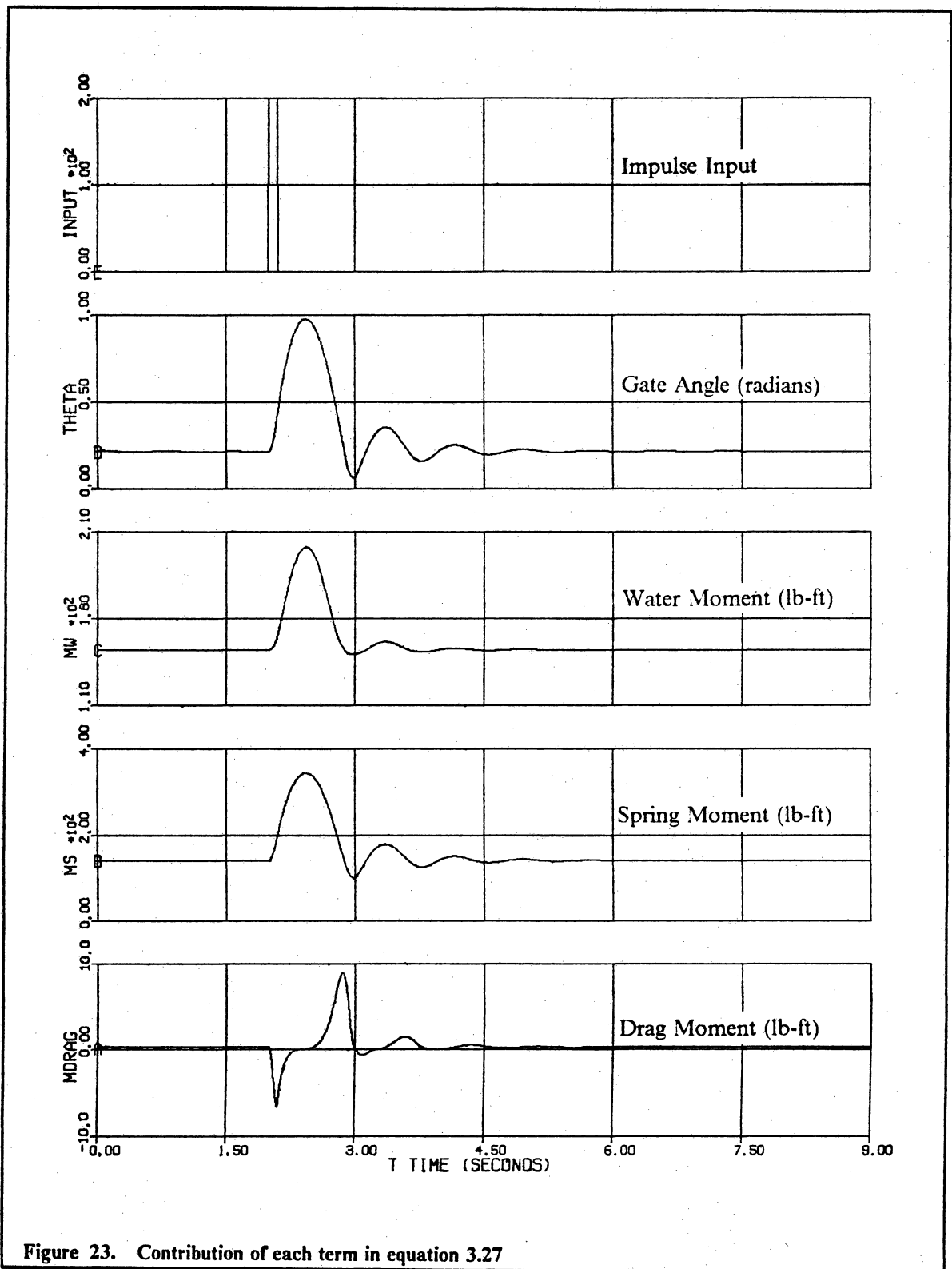


Figure 23. Contribution of each term in equation 3.27

bottom Figure 24 shows: the impulse input; a low water response (initial water height = 2.5 ft, initial gate angle = 14.3°), a medium water response (initial water height = 3.0 ft, initial gate angle = 32.6°), and a high water response (initial water height = 3.5 ft, initial gate angle = 56.7°). Figure 24 shows that as water height increases, the response of the gate is slower due to the greater effective inertia caused by the surrounding water.

3.4.2 Slow Model

The first order model is used to investigate water level and gate response to extended periods of rain for various rain time histories. This is to demonstrate that as the water level rises the gate opens and as the rain stops, the gate slowly returns to its normal position. This section presents a sample of typical results obtained from simulations using the first order model. Two figures are presented which show the water height response, gate angle response, and flow over the gate for two hypothetical rain time histories. From top to bottom, Figure 25 shows the hypothetical rain history, the water height response, the gate angle response, and the flow over the gate. Figure 26 presents similar results for a different rain input. Note that the time scale is in hours now. A two foot gate of unit width, lake area of one acre, and drainage area of four acres was assumed in the simulation.

3.4.3 Optimum Gate Height

In the preceding models, the ratio of gate height to flood rights ($\frac{GH}{FR}$) was taken to be $\frac{1}{2}$. The third order (fast) model was used to investigate the consequences of increasing this ratio in an attempt to make use of as much of the available water storage area as possible.

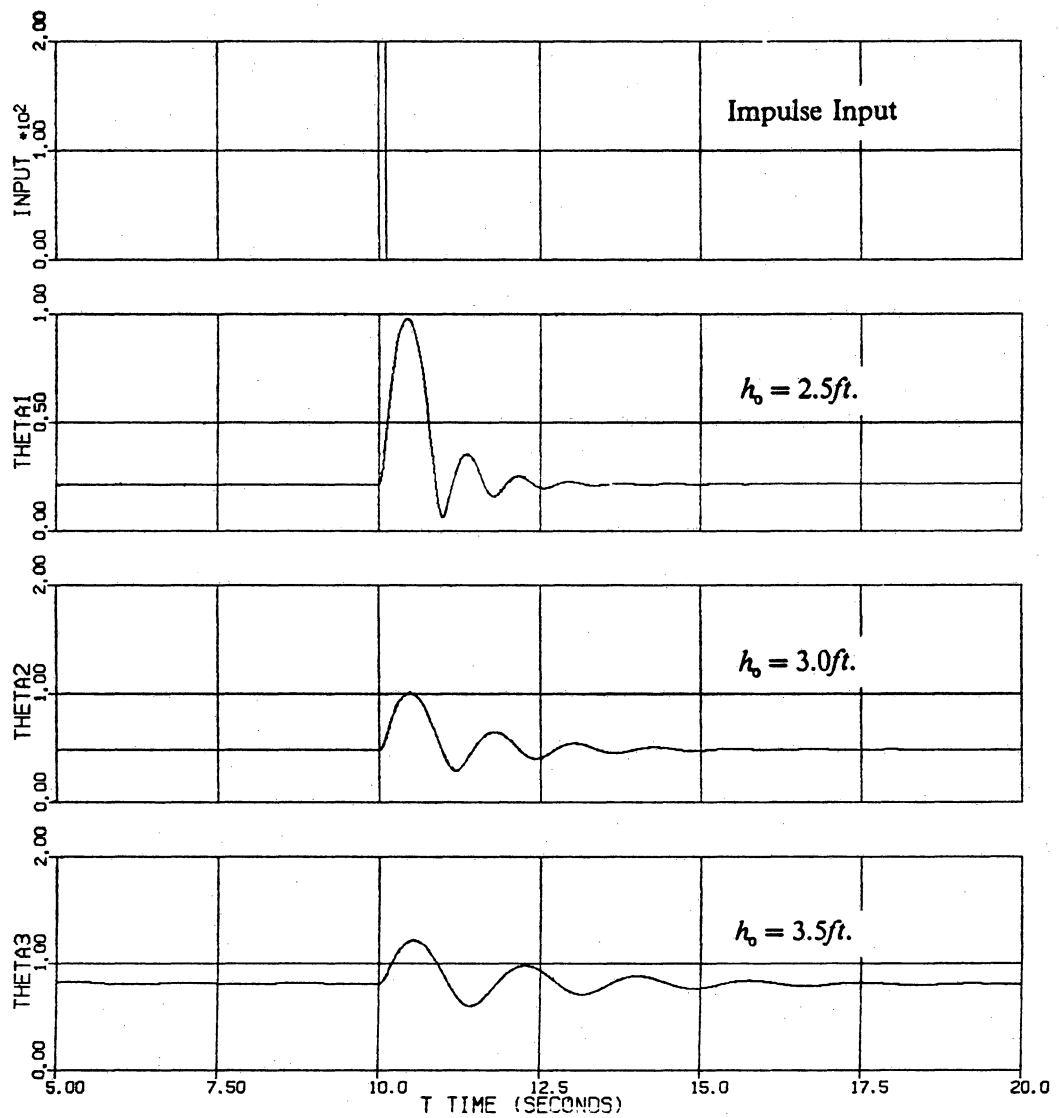


Figure 24. Three water level response to impulse

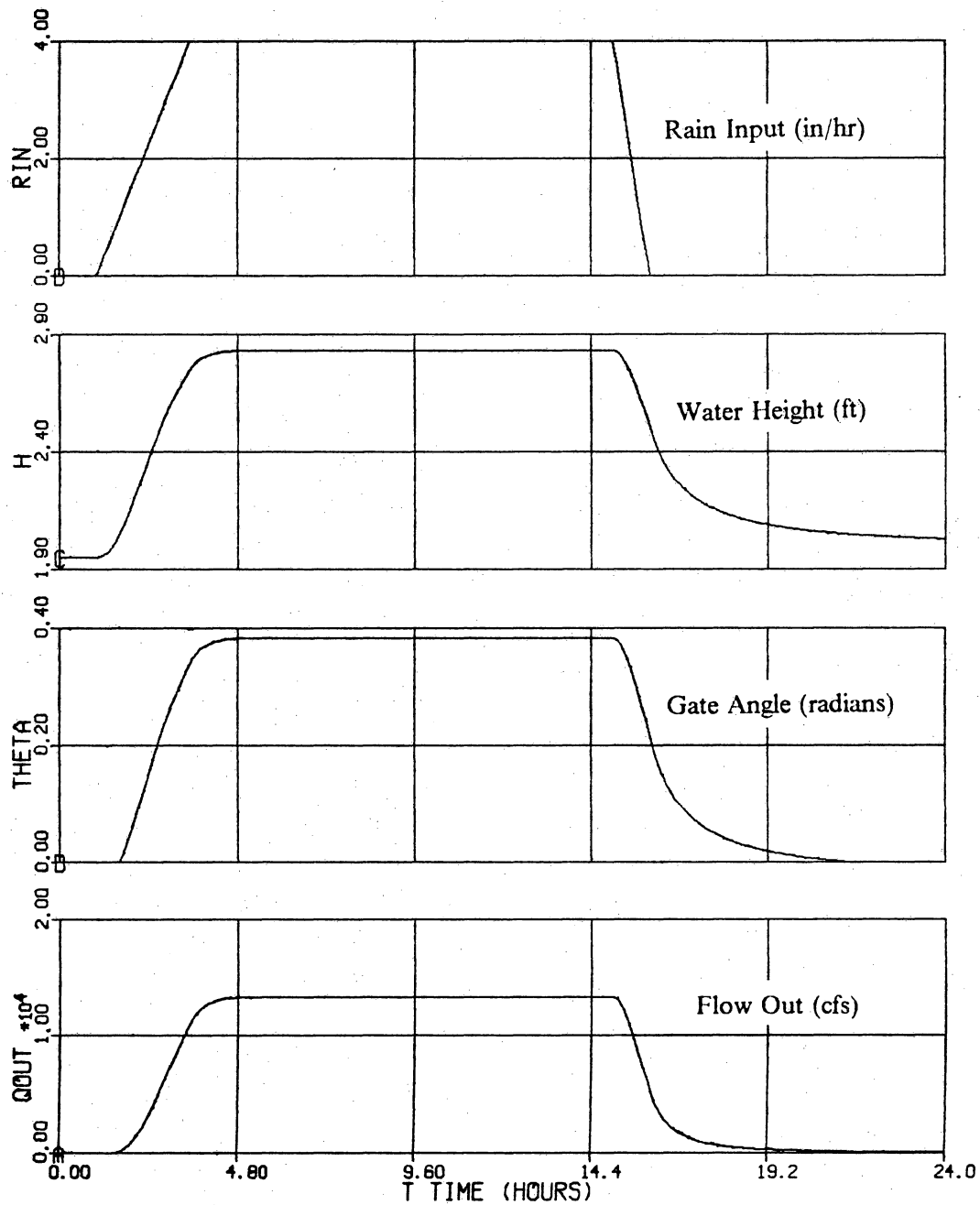


Figure 25. First order model response to rain input 1

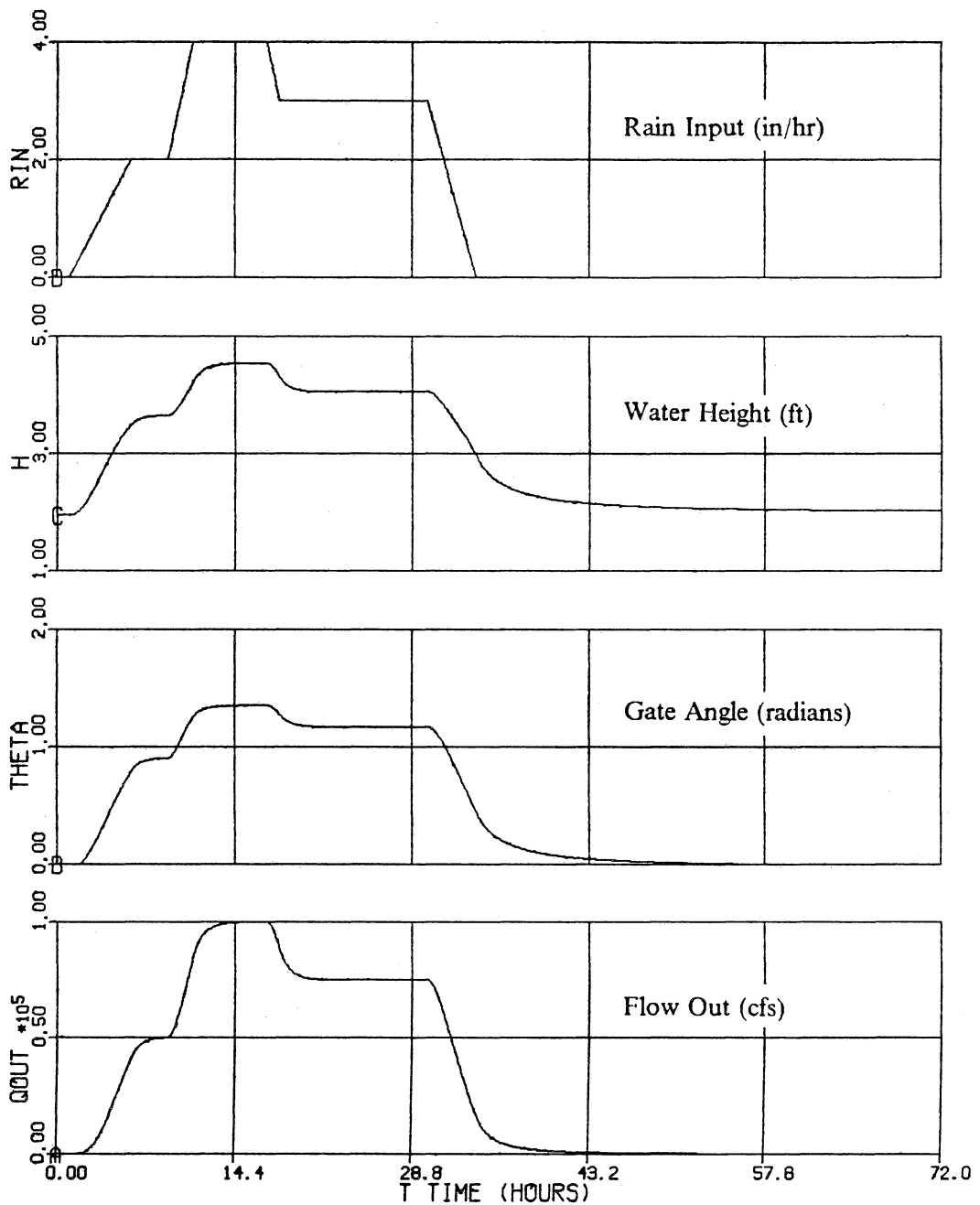


Figure 26. First order model response to rain input 2

As the gate height to flood rights ratio approached unity, a "bang-bang" phenomenon was noted in the gate response. Bang-bang response is defined as rapid opening and closing of the gate. To investigate the cause of this phenomenon, the spring rate equation (3.20) was normalized to the gate height to flood rights ratio. This normalization gives:

$$\frac{K}{FR^3} = \frac{\gamma}{\pi} \left(\frac{GH}{FR} \right)^2 \left[1 - \frac{1}{3} \left(\frac{GH}{FR} \right) \right] \quad (3.36)$$

Likewise, the required spring preload angle as a function of the gate height to flood rights ratio is found to be:

$$\theta_o = \frac{\frac{\pi}{6} \left(\frac{GH}{FR} \right)}{\left[1 - \frac{1}{3} \left(\frac{GH}{FR} \right) \right]} \quad (3.37)$$

Equations (3.36) and (3.37) are used with the moment equations (3.8) and (3.9) to plot gate angle versus water height for increasing gate height to flood rights ratio. The results are shown in Figure 27. The ratio of gate height to flood rights is increased from 0.5 to 1.0.

Note that as the ratio of gate height to flood rights is increased two equilibrium points are possible. For instance for $\frac{GH}{FR} = 1$ the gate could be vertical or horizontal at a water depth of 4 feet (see Figure 27). The occurrence of multiple equilibrium points can explain the bang-bang action of the gate as the gate height to flood rights ratio is increased.

The theoretical optimum gate height is then the gate height that gives the maximum gate height to flood rights ratio without multiple equilibrium gate positions. The maximum gate height to flood rights ratio without multiple equilibrium points is the ratio that gives an infinite slope at $\theta = 90^\circ$ as in Figure 27

$$\left. \frac{\partial \theta}{\partial h} \right|_{\theta=90^\circ} = \infty$$

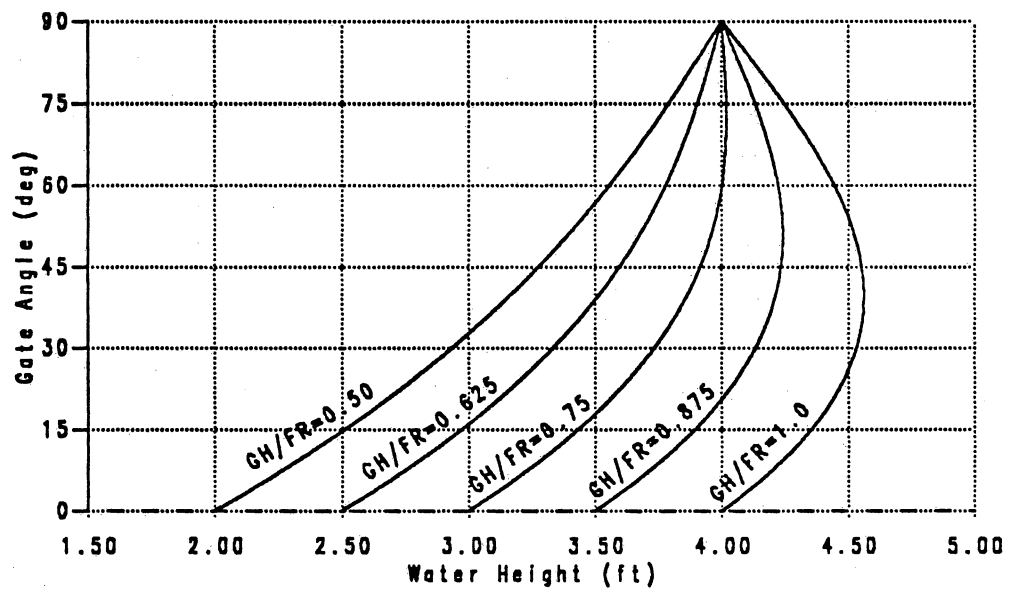


Figure 27. Gate angle vs. water height for gate height to flood right ratios

or equivalently,

$$\left. \frac{\partial h}{\partial \theta} \right|_{\theta=90^\circ} = 0$$

Taking the partial of h with respect to θ and setting equal to zero gives:

$$\frac{2}{GH^2} \left[\frac{K_t}{\gamma} - \frac{GH^3}{3} \sin \theta \right] = 0$$

Next, the normalized spring rate equation (3.36) is substituted for K_t . Solving for the gate height to flood rights ratio using a gate angle of $\theta = 90^\circ$ gives:

$$\left(\frac{GH}{FR} \right) = \frac{3}{\pi + 1} \quad (3.38)$$

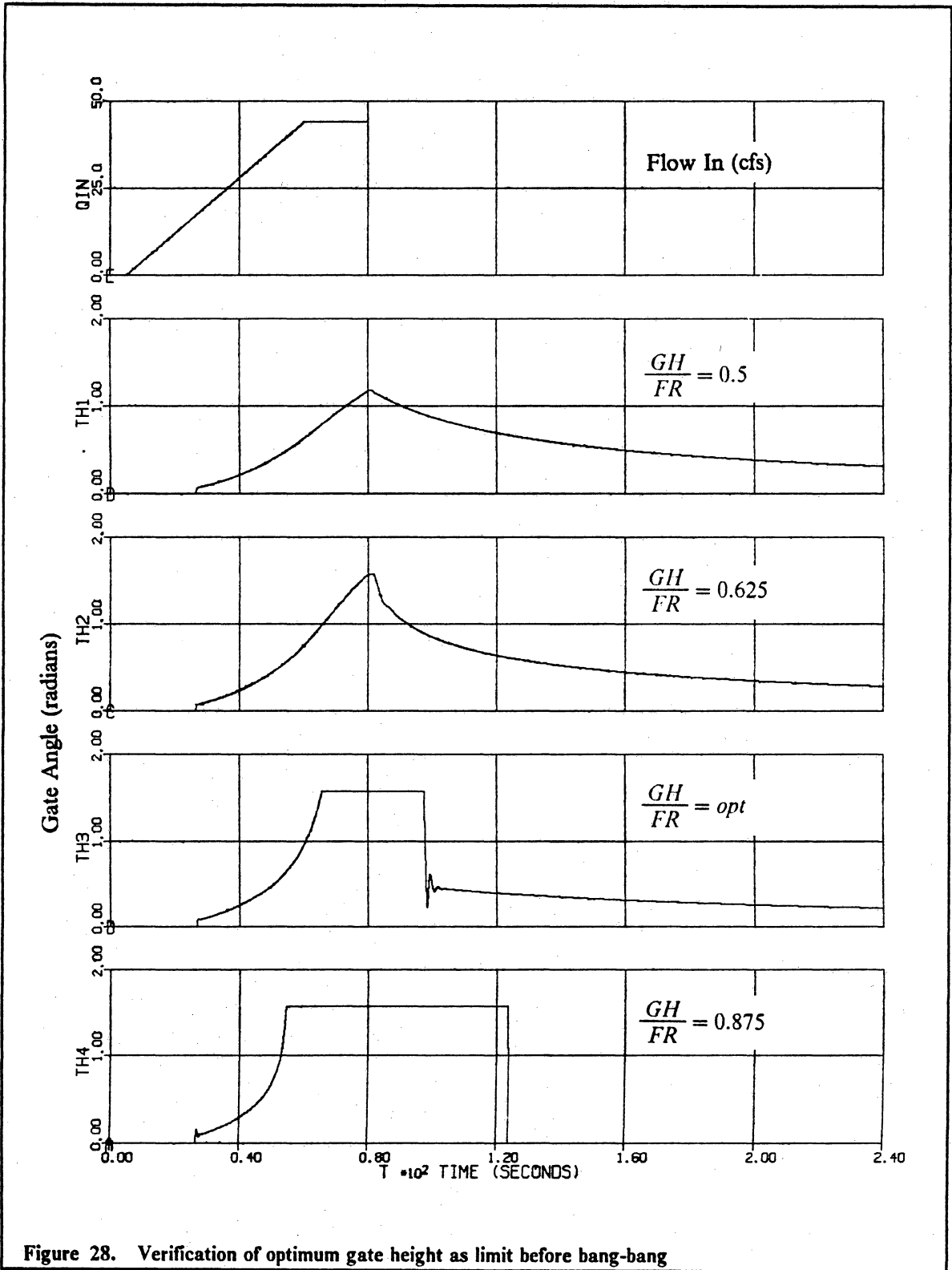
Equation (3.38) is the maximum gate height to flood rights ratio to avoid multiple equilibrium points of the gate. The theoretical optimum gate height for a given flood rights level is then:

$$GH_{\text{opt}} = \frac{3}{\pi + 1} FR \quad (3.39)$$

Gate heights greater than this will cause a bang-bang type of gate response.

To verify equation (3.39) as the limiting gate height before bang-bang occurs, the third order simulation model was run using a gate height at this limiting height along with gate heights lower and higher than the optimum. The results of this simulation are shown in Figure 28.

From top to bottom are: the flow input, gate response of lower gate; optimum gate; and higher gate. Notice that at the optimum gate height the response is starting to ring and with the higher gate the response exhibits the undesirable bang-bang response. The response of the theoretical optimum gate height is still too "jerky" to be considered optimum. This is explained by the fact that the theoretical optimum gate height was based on a static analysis. There is no closed form algebraic way to determine the dynamic optimum gate height. The third order model can be used to iter-



actively determine the dynamic optimum gate height. This was done with the same model parameters used in the previous model and the results are shown in Figure 29. Because of the installation dependant uncertainties in the dynamic model a factor of safety should be applied when choosing a gate height. Chapter 5 discusses alternatives that influence this design parameter.

Another consideration when choosing the optimum gate height is that the flood rights level is not exceeded. As the gate height is raised and more of the flood volume is used, there is the possibility of exceeding the flood rights level. Flood rights can be exceeded if the maximum inflow is sufficiently large and occurs over a long enough time period. The gate can be horizontal and because of the greater volume of stored water the Flash Gate Board may not allow for enough discharge to prevent the water from exceeding the flood rights level. The determining factors in this are the crest length, the lake area, and the maximum expected inflow volume and duration. The slow model can be used to verify an optimum gate height for a given reservoir. If the flood rights is exceeded then the gate height must be reduced. This process is repeated until a satisfactory gate height is found.

The two models above were incorporated into a dynamic simulation tool for designers. The software was written in FORTRAN to run on an IBM-PC. This software and a user's guide are available from the VPI & SU Mechanical Engineering Department.

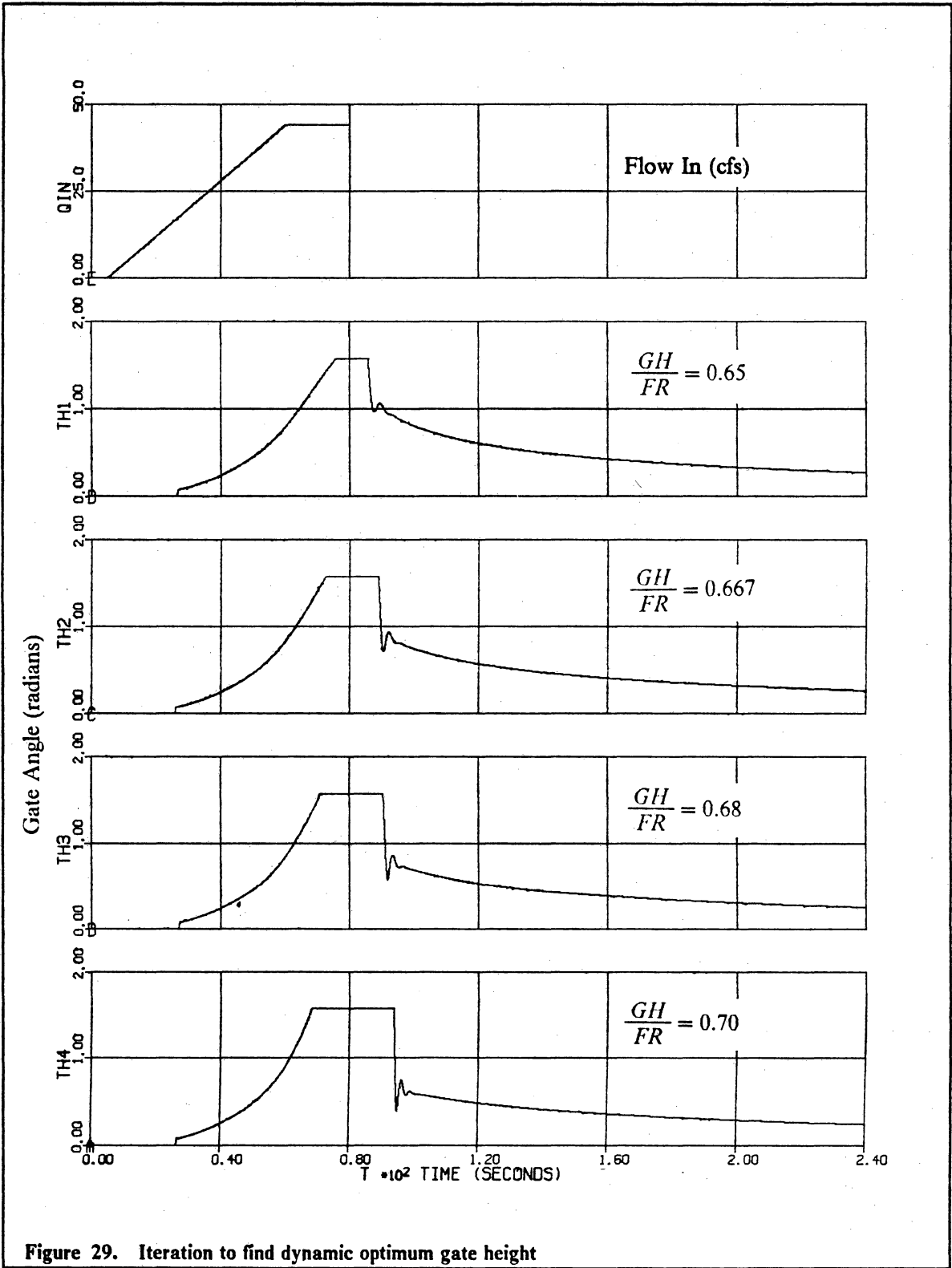


Figure 29. Iteration to find dynamic optimum gate height

4.0 Experimental Analysis

A small scale ($\approx 1:30$ based on a 2 foot gate height) experimental model of the Flash Gate Board was built to qualitatively verify the results from the analytical work. The main purpose of the model was to verify that the Flash Gate Board does indeed behave as expected. This section explains the construction of the experimental model, describes the experiment and discusses the conclusions that can be drawn from this qualitative experiment. Suggestions for future experimental testing are also discussed.

4.1 *Experimental Setup*

A dimensional analysis was performed to determine the important parameters in the model. Of the dimensionless groups obtained, the Froudian criterion (Froude Number) is most important for free surface flows because gravitational effects dominate (Sharp, 1981 [17]). Thus, the scale of the model was chosen by considering the size of the available water table combined with the Froudian (or gravitational) similarity criterion.

One gate section was used because the flow is largely two-dimensional and there are no major variations in flow patterns from one gate to another. The experiment was conducted on a five by two foot water table. The main components include:

1. $4" \times \frac{3}{4}"$ plexiglass gate section with $\frac{1}{8}"$ drill rod for the gate pins.
2. $4" \times 4"$ plexiglass gate side plates fixed to a mounting bracket.

3. Torsion bar restoring spring made from 0.018" music wire.
4. Removable gate pier sections

An exploded view of these components is shown in Figure 30. The gate side plates were designed to be adjustable to facilitate installation and removal of the gate. Holes drilled in the plexiglass side plates serve as bearings for the gate pins. The holes were polished to reduce friction. The side plate mount was fitted with an adjustable gate stop. The gate stop was used in conjunction with an adjustable lever arm that attached to the gate pin in place of the restoring spring. Using the gate stop, the lever arm, and a spring scale, the actual moment due to the water was determined. The details of this determination are discussed in the next section.

The pier sections were designed after the round nose type 2 piers discussed in chapter 3. Removable piers were used to examine the effects on flow and gate response with and without piers.

The restoring spring is a torsion bar spring made from music wire. The spring was designed using the criteria outlined in section 3.2.5.1. The restoring spring was fitted with an adjustable fixed end to enable preload adjustment. The use of a torsion bar spring is permissible because of the small scale of the model and because infinite life of the spring is not required.

The flow source for the model was provided by a centrifugal pump. The flow is supplied through a flow diffuser to provide smooth input flow. A scale was used to measure the depth of water upstream of the gate. Duct tape was used for the gate bottom seal and no side seals were used.

4.2 Operation of Experiment

The restoring spring was removed from the model and the lever arm installed. The adjustable gate stop was used to set the gate angle. The water level in the tank was stabilized and a spring scale

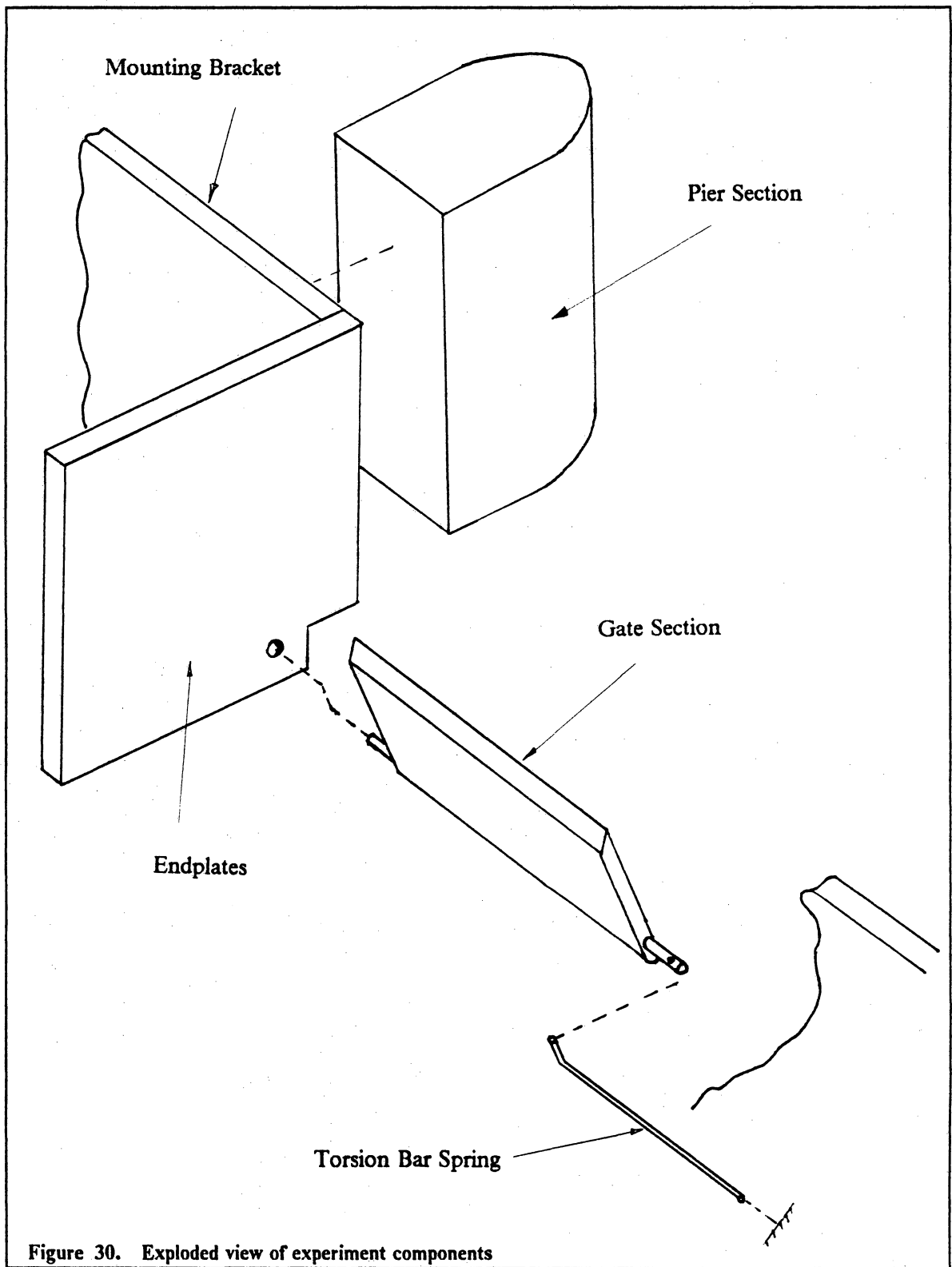


Figure 30. Exploded view of experiment components

was used to measure the force due to the flowing water on the lever arm. Knowing the force and the lever length, the actual moment was then calculated. This was done to qualify the moment coefficients derived in section 3.2.3.

The operation of the experimental Flash Gate Board was first checked by slowly increasing the water level in the tank and noting the response of the gate. Next, the inflow was completely turned off and again the gate response observed. Similar runs were made with and without the piers attached.

The model was also used to examine the gate response to an impact. A steady gate position and tank water height position were first obtained. A block of wood approximately $1" \times \frac{1}{2}"$ was then dropped on the gate from above to examine the transient response of the gate.

Finally, an experiment was conducted to investigate wave effects on the system. Waves were induced on the surface of the test tank and the gate response observed.

4.3 Experimental Results and Observations

First the actual moment at the gate pin due to the flowing water was checked to verify the moment coefficients. The actual moment was determined using the procedure described above at gate angles of 0° , 45° , and 90° . The actual measured moment was within 5 % of the estimated value using equations 3.8 ($\theta = 0^\circ$) and 3.9 with the moment coefficients ($\theta = 45^\circ$ and $\theta = 90^\circ$). Although this indicates the moment coefficients are an acceptable measure of the actual moment on the gate, the precision of the spring scale and small scale of the model are not considered good enough for a true test of the calculated moment coefficients. Further tests of this kind need to be performed to accurately quantify the moment coefficients.

The general operation of the experimental gate was as expected. With increasing water depth the gate begins to open. As the water depth reaches the maximum, the gate is nearly horizontal (fully opened). After the inflow is turned off, the gate raises as the water level in the tank drops. However, because of the small scale of the model, friction effects caused some problems. The phenomenon of "stiction" was observed. This causes the gate to "stick" at intermediate positions until the static friction force is overcome by the force of the spring and water. Separating the gate side plates slightly helped to alleviate this problem. Including better bearings in the model would no doubt also reduce this problem. It is hard to compare the friction effects noted in this model to an actual full-size gate. Friction does not scale with size.

The importance of piers on the operation of the Flash Gate Board system was indicated by the model. With the piers in place, the contraction of the nappe was smooth and uniform. Removing the piers, leaving only the sharp edge of the side plate caused a sudden contraction of the nappe due to the increased contribution of the lateral flow effects. The severity of this sudden contraction increased with increasing gate angle.

The gate response to the impact was also as expected. Following impact, the gate responded by quickly opening and then returning to its initial state before impact with a single slight overshoot. This verifies that the dynamic simulation results with a damping ratio of 0.1 were conservative.

In the surface wave experiment, the gate responded, but no indication of sustained oscillations were observed. The gate seemed to be "slower" than the typical surface wave.

The small scale qualitative experiment performed serves only as a prelude to more elaborate experimental testing. A hydroelastic scale model built with greater precision and properly equipped with the necessary instrumentation would provide quantitative experimental results to enable direct comparison with the analytical results of Chapter 3. Recommendations for further experimental testing are discussed in the next chapter.

5.0 Conclusions and Recommendations

Analytical and experimental models of the Flash Gate Board have been developed and used to demonstrate the operation of the device. The analytical and experimental analysis performed indicates the use of the Flash Gate Board is an effective means of regulating the surface and extending the crest height of an overflow dam. This chapter draws conclusions from the study, discusses possible extensions to the analytical model, makes recommendations for future work, and discusses important design considerations.

The static analysis provided equations for the moment at the gate pin and for flow over the gate. These equations were used in determining the static behavior of the gate. Based on the results of the static analysis of the Flash Gate Board, it was determined that a linear torsional spring can be used to provide the necessary restoring torque to the gate. This result is significant because linear springs are simpler and more economical to manufacture. Compared to the torsion bar spring, the helical torsion spring provided greater design flexibility while satisfying the requirements for a safe design.

The dynamic analysis provided two models for studying Flash Gate Board behavior. The results of the first order (slow) model show that the Flash Gate Board operates as designed. As the water level reaches or nears the flood rights level, the gate opens allowing for passage of flood water. When flood water recedes, the gate returns to its normal position (upright for this study).

Based on the results of the third order (fast) model a theoretical optimum gate height was derived using a static formulation. A static formulation was used so that a closed-form solution could be found. This optimum gate height is the theoretical upper limit for the Flash Gate Board gate height

before multiple equilibrium points occur. Above this height, unfavorable (bang-bang) gate behavior occurs.

This value of optimum gate height is not the true optimum value because it is based on a static formulation. A closed-form solution for the dynamic optimum gate height does not exist. The third order analytical model was used to iteratively find an optimum gate height where acceptable dynamic behavior is realized. This method can be implemented using the software developed to determine the optimum gate height for a given installation. However, the optimum height found using this procedure may not directly coincide with the heights of manufactured gates. In such instances, the optimum value should be rounded down to the next available gate height.

Based on the third order model, it can also be concluded that the Flash Gate Board exhibits an acceptable dynamic response to impulsive loads. However, because of the inability to accurately describe the contribution of seal and bearing friction to the damping coefficient, the actual results will not likely mirror the results of the analytical simulation. This is evident from the results of the experiment. Friction was a determining factor in the observed experimental gate response. However, in the analytical model, friction was assumed to be minimal.

While the qualitative experiment provided close verification for the results of the static analysis, the results of the dynamic analysis are not as closely verified. While fundamentally the same, the analytical model exhibits characteristics of a lightly damped system whereas the experimental model has the characteristics of a system with considerably more damping. This discrepancy represents the greatest amount of uncertainty in the analytical model. Increasing the damping coefficient in the analytical model will result in a response more representative of actual results. Adding coulomb damping to the model would also help.

Only linear viscous mechanical damping is assumed in the current model. The experimental results indicate a stiction effect exists. Modifying the model to include stiction effects may result in a more accurate representation. Other modifications to the model may be added. These modifications

involve a more detailed treatment of the fluid mechanics. However, while these modifications will provide a more thorough treatment, they may not necessarily produce a better model. The fundamental behavior of the system should not change.

The following list of possible extensions to the analytical model all involve improved treatment of the fluid mechanics.

- A more detailed model of the reservoir can be implemented. The assumption of uniform water height was made in deriving the reservoir model. This does not allow for the study of the surface conditions of the reservoir or for the interaction between multiple gate sections due to water coupling. In order to consider water surface effects in the analytical model, a high order, multiple control volume approach must be used. This approach can result in computational difficulties because of the high order of the model and the small time step needed.
- In this study a hydrostatic pressure distribution was assumed to find the moment at the gate pin due to the upstream water. Implementing a potential flow field to determine the pressure distribution provides a more accurate formulation. The potential flow formulation assumes a stationary body. Therefore, several formulations and solutions are needed to describe the pressure distribution for each position of the gate at a given water depth and velocity. Particular attention should be directed at studies of the flow when the gate is near the horizontal position.
- The virtual inertia of the gate could be refined using one of the methods presented in section 3.3.1.1. Again, these methods will be computationally intensive.

When modeling a physical phenomenon with simulation methods, two main considerations are computational accuracy and cost. The phenomenon must be described with sufficient accuracy and the computation performed at a low enough price to make it worthwhile. Usually accuracy and

cost are opposing constraints. Still some assumptions must be made to implement the extensions to the analytical model listed above.

The improved accuracy to be gained by these methods is "unknown". These extensions to the analytical model should only be made in conjunction with an in-depth experimental study to verify the analytical results. In particular the actual moment on the gate needs to be accurately measured to ensure proper design of the spring and operation of the gate.

Based on the above discussion it is recommended that a study using a precise hydroelastic prototype model be carried out. This study should investigate all possible effects on the system to verify proper operation before initiating full-scale production. The interaction between gate sections and wave effects could be more thoroughly studied with an experimental model. The reliability of the Flash Gate Board system also needs to be carefully considered and studied. However, no analytical model or experimental prototype study can predict the effects of wear and corrosion or ice on the system.

It is also recommended that ventilation of the nappe and proper seal design be considered in the final design of the Flash Gate Board. Proper ventilation of the air space under the nappe is critical for a vibration free design. If at all possible, the Flash Gate Board should be installed so that natural ventilation is obtained. When conditions do not allow for natural ventilation, one of the following methods may be used.

- Fixed vertical gate sections can be installed at both ends of the dam crest. These end sections will allow ventilation to occur at the ends of the dam crest. More ventilation is provided as the length of these fixed ends is increased. Ventilating with this method does however, greatly reduce the effective crest length of the dam.
- Nappe splitters (or spoilers) provide an efficient means of adding ventilation with minimal design change. The nappe splitters separate the overflowing water thus ventilating the

trapped air under the nappe. Several types of nappe splitters have been used successfully. The proper spacing of the splitters and the best type for use on the Flash Gate Board will depend on the specific installation. Using nappe splitters is the recommended method for ventilating the nappe.

- Additional ventilation of the air space under the nappe can be provided by use of aeration pipes. Aeration pipes can be installed in the pier sections between the gates. The upper end of the aeration pipe must always be above the water line.

Proper design of the pier sections may provide the required ventilation to prevent nappe oscillation. However, the pier sections must be carefully designed to avoid unfavorable approach flow conditions and a reduced effective crest length. The design of pier sections is an important design consideration that should not be overlooked. However, while pier design is beyond the scope of this work, the proper design of gate piers is thoroughly covered in the literature.

The seals of the Flash Gate Board must also be carefully designed or chosen in order to prevent problems with seal vibration. The side seals should be designed to maintain contact with the side plates at all times. To facilitate this, the seal must be flexible, and all possible causes of side seal gap (*i.e.* inaccurate construction, temperature shrinkage, structural settlements, etc.) must be considered in the initial design or selection phases. If large gaps are anticipated, Schmidgalls side seal design is a possible alternative. The bottom seal must be designed so that no debris can get lodged under the seal. More information about the proper design of seals can be found in the literature.

In conclusion, the results of this study suggest the Flash Gate Board concept is sound. However, care must be taken in the implementation of real hardware. The degree of success realized will depend on proper installation and design of the gate mountings. It is recommended that a working prototype be developed or a full size field test be made. As with all automatic crest gates, operation should be closely monitored during flood conditions.

References

1. Blevins, Robert D., *Flow-Induced Vibration*, Robert E. Krieger Publishing Company, Malabar, Florida, 1986.
2. Campbell, Frank B., "Vibration Problems in Hydraulic Structures," *Journal of the Hydraulics Division, Proceedings of ASCE*, Vol. 87, No. HY2, March 1961, pp. 61-77.
3. Chen, Pah-i, "The Effect of Sloping the Upstream Face of Rectangular Weirs Upon Nappe Shape," Thesis, Virginia Polytechnic Institute, November 1963.
4. Chow, Ven Te, *Open-Channel Hydraulics*, McGraw-Hill Book Company, New York, 1959.
5. Creager, W. P., Justin, J. D., and Hinds, J., *Engineering for Dams, Volume III*, John Wiley and Sons, Inc., New York, 1928.
6. Creager, W. P., Justin, J. D., *Hydro-Electric Handbook*, John Wiley and Sons, Inc., New York, 1927.
7. Davis, Calvin V., ed. and Sorensen, Kenneth E., co-ed., *Handbook of Applied Hydraulics 3rd ed.*, McGraw-Hill Book Company, New York, 1969.
8. Homma, M., and Ogihara, K., "Theoretical analysis of flap gate oscillation," 17th IAHR Congress, Baden-Baden, 1977, vol. 4, paper C51.
9. Imaichi, Kensaku, and Ishii, Noriaki, "Instability of an Idealized Taintor-Gate system without damping caused by Surface Waves on the Backwater of Dam," *Bulletin of the JSME*, vol. 20, No. 146, August, 1977, pp. 963-970.
10. Johnson, William M., "Flash Gate Board", unpublished notes dated March 11, 1980.
11. Kolkman, P. A., "Development of Vibration-Free Gate Design: Learning from Experience and Theory," Publication No. 219, Delft Hydraulics Laboratory, Netherlands, November 1979.

12. Mcguire, Bernard, "Final Technical Review; Flash Gate Board," *OERI NUMBER: 10826*, April 1986.
13. Mitchell and Gauthier, *Advanced Continuous Simulation Language (ACSL) Reference Manual 4th ed.*, Mitchell and Gauthier Associates, Concord, Mass., 1986.
14. Naudascher, E. and Rockwell, D. (Eds.), *Practical Experiences with Flow Induced Vibrations*, IAHR/IUTAM Symp. Karlsruhe 1979, Springer Verlag, Berlin, 1980.
15. Neilson, Frank M. and Pickett, Ellis B., "Corps of Engineers Experiences with Flow-induced Vibrations," in reference 14, IAHR/IUTAM Symp. Karlsruhe 1979.
16. Novak, P., ed., *Developments in Hydraulic Engineering Vol 2*, Elsevier Applied Science Publishers, London, 1984.
17. Ogihara, K, and Udea, S., "Flap Gate Oscillation," in reference 14, IAHR/IUTAM Symp. Karlsruhe 1979.
18. Petrikat, Kurt, "Seal Vibration," in reference 14, IAHR/IUTAM Symp. Karlsruhe 1979.
19. Pickwell, Richard A., "Effects of Boat Wakes on the Shoreline of Lake Manapouri," *New Zealand Engineering*, vol. 33, no. 9, September 1978.
20. Schmidgall, Tasso M., "Spillway Gate Vibrations on the Arkansas River," *Journal of the Hydraulics Division, Proceedings of ASCE*, Vol. 98, No. HY1, January 1972, pp. 219-238.
21. Schwartz, H. Ivan, "Nappe Oscillation," *Journal of the Hydraulics Division, Proceedings of ASCE*, Vol. 90, No. HY6, November 1964, pp. 129-143.
22. Shames, Irving H., *Mechanics of Fluids 2nd ed.* McGraw Hill, New York, 1982.
23. Sharp, J. J., *Hydraulic Modelling*, Butterworths, London, 1981.
24. Shigley, J. E. and Mitchell, L. D. *Mechanical Engineering Design*, McGraw-Hill Book Company, New York, 1983.
25. Streeter, Victor L. and Wylie, E. Benjamin, *Fluid Mechanics 8th ed.*, McGraw-Hill Book Company, New York, 1985.
26. Zienkiewics, O. C. and Nath. B., "Analogue procedure for determination of virtual mass," *Journal of the Hydraulics Division, Proceedings of ASCE*, Vol. 90, No. HY5, September 1964, pp. 69-81.

**The vita has been removed from
the scanned document**